

# Theoretical Limitations on the Broadband Matching of Arbitrary Impedances

R. M. FANO

TECHNICAL REPORT NO. 41

January 2, 1948

RESEARCH LABORATORY OF ELECTRONICS  
MASSACHUSETTS INSTITUTE OF TECHNOLOGY

The research reported in this document was made possible through support extended the Massachusetts Institute of Technology, Research Laboratory of Electronics, jointly by the Army Signal Corps, the Navy Department (Office of Naval Research), and the Army Air Forces (Air Materiel Command), under the Signal Corps Contract No. W-36-039 sc-32037.

MASSACHUSETTS INSTITUTE OF TECHNOLOGY  
Research Laboratory of Electronics

Technical Report No. 41

January 2, 1948

THEORETICAL LIMITATIONS ON THE BROADBAND MATCHING  
OF ARBITRARY IMPEDANCES

by

R. M. Fano

Abstract

This paper deals with the general problem of matching an arbitrary load impedance to a pure resistance by means of a reactive network. It consists primarily of a systematic study of the origin and nature of the theoretical limitations on the tolerance and bandwidth of match and of their dependence on the characteristics of the given load impedance. Necessary and sufficient conditions are derived for the physical realizability of a function of frequency representing the input reflection coefficient of a matching network terminated in a prescribed load impedance. These conditions of physical realizability are then transformed into a set of integral relations involving the logarithm of the magnitude of the reflection coefficient. Such relations are particularly suitable for the study of the limitations on the bandwidth and tolerance of match. Definite expressions for these quantities are obtained in special cases. The practical problem of approaching the optimum theoretical tolerance by means of a network with a finite number of elements is also considered. Design curves are provided for a particularly simple but very important type of load impedance. In addition, a very convenient method is presented for computing the values of the elements of the resulting matching network.

---

\* The work presented in this paper is part of a thesis with the same title submitted by the author in partial fulfillment of the requirements for the degree of Doctor of Science at the Massachusetts Institute of Technology (June 1947). A summary was presented to the National Electronics Conference in Chicago on November 3, 1947.



## THEORETICAL LIMITATIONS ON THE BROADBAND MATCHING OF ARBITRARY IMPEDANCES

### 1. The Matching Problem

The transfer of power from a generator to a load constitutes one of the fundamental problems in the design of communication systems. A problem of this type involves in every case the design of a lossless coupling network to transform a given load impedance into another specified impedance. One refers to this operation as "impedance matching". In most practical cases this problem can be idealized as indicated in Fig. 1. The

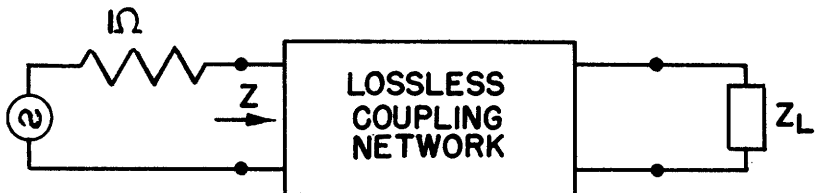


Figure 1. Matching network for an arbitrary load impedance.

generator is assumed to consist of an ideal voltage source in series with a pure resistance; maximum power transfer is then obtained when the impedance presented to the generator is equal to the source resistance.

It will be shown later that it is not possible to match an arbitrary impedance to a pure resistance over the whole frequency spectrum, or even at all frequencies within a finite frequency band. On the other hand, it is evidently possible to obtain a match at any desired number of frequencies, provided the given impedance has a finite resistive component at those frequencies. Such a matching, however, has little practical value because it is incorrect to assume that one can obtain a reasonable match over a frequency band by correctly matching at a sufficiently large number of frequencies within the desired band.

It becomes clear at this point that the statement of any matching problem must include the maximum tolerance on the match as well as the minimum bandwidth within which the match is to be obtained. Furthermore, it is reasonable to expect that, for a given load impedance and a given maximum tolerance, there is an upper limit to the bandwidth that can be obtained by means of a physically realizable coupling network. It follows

that an investigation of such a limit should be the first step in any systematic study of matching networks. Before this problem can be stated in a precise manner, however, one must define an appropriate measure of the match so as to give to the tolerance a definite quantitative meaning.

In view of the fact that matching is used to maximize the load power, it appears reasonable to measure the match in terms of the actual load power  $P_L$  divided by the maximum power  $P_o$  that could be delivered by the generator. Actually, the most convenient quantity for this purpose is the per unit power rejected by the load, that is

$$|\rho|^2 = 1 - \frac{P_L}{P_o} . \quad (1)$$

It will be recognized that  $\rho$  is the reflection coefficient defined by

$$\rho = \frac{Z-1}{Z+1}$$

where  $Z$  is the impedance presented to the generator as indicated in Fig. 1.\* If the generator were connected to the coupling network by a transmission line of characteristic impedance equal to the source resistance, the voltage standing-wave ratio on the line would be given by

$$\text{VSWR} = \frac{1+|\rho|}{1-|\rho|} . \quad (2)$$

The problem of the broadband matching of an arbitrary impedance can now be stated as follows. With reference to Fig. 1,  $Z_L$  is a given impedance function of frequency, subject only to the restriction of being realizable by means of a finite number of linear passive elements. A non-dissipative coupling network must be designed such that, when terminated in  $Z_L$ , the magnitude of the input reflection coefficient is smaller than, or equal to, a specified value  $|\rho|_{\max}$  at all frequencies within a specified band.

The exclusion from the system of distributed-constant elements such as transmission lines, cavity resonators, etc., is required by the fact that the available techniques of network analysis and synthesis are limited to lumped-element systems. Such a limitation, however, is not so serious as it may appear at first because, in many practical cases, the results obtained in the case of lumped-element networks can be extended, in an approximate fashion, to the case of distributed-constant systems. For instance, such a technique has been successfully employed by the author in the design of microwave filters.<sup>1</sup>

\* In Fig. 1 as well as in the rest of this paper all the impedances are normalized with respect to the source resistance unless otherwise stated.

<sup>1</sup> See references p. 34.

An additional remark must be made on the fact that the coupling network is assumed to be lossless. In practice, of course, a certain amount of incidental dissipation will be present, which will result in a distortion of the characteristics of the coupling network. Techniques for computing this distortion and correcting for it have been developed in connection with the design of filters<sup>2,3</sup>. It seems appropriate, therefore, to neglect the presence of losses in the following analysis, and to rely on the available techniques for any correction that might become necessary in the final stage of a particular design.

Matching networks have been designed in the past following a step by step procedure leading to a ladder structure of reactances. Such a procedure has two main weaknesses. In the first place the designer does not know whether the requirements that he is trying to meet are consistent with the given load impedance. In the second place, it is implicitly assumed that a process based on successive improvements converges to the optimum design, or, at least, to a design reasonably close to the optimum. This is not the case, in general. An improved procedure of the same type, suggested by Bode<sup>4,5</sup> in 1930 suffers still from most of the same weaknesses.

The first step toward a systematic investigation of matching networks was made by Bode<sup>6</sup> some time later, in connection with a very special but important type of load impedance. He considered the case of an impedance consisting of a resistance R shunted by a capacitance C, and showed that the fundamental limitation on the matching network takes the form

$$\int_0^\infty \ln \frac{1}{|\rho|} dw \leq \frac{\pi}{RC} \quad (3)$$

where  $\rho$  is the input reflection coefficient corresponding to the impedance  $Z$  in Fig. 1. If  $|\rho|$  is kept constant and equal to  $|\rho|_{\max}$  over a frequency band of width  $w$  (in rad. per sec.) and is made equal to unity over the rest of the frequency spectrum, Eq. (3) yields

$$w \ln \frac{1}{|\rho|_{\max}} \leq \frac{\pi}{RC} . \quad (4)$$

In words, the product of the bandwidth by the minimum pass-band value of  $\ln 1/|\rho|_{\max}$ , has a maximum limit fixed by the product  $RC$ . Equation (3) indicates also that approaching a perfect match, that is, making  $|\rho|$  very small at any frequency, results in an unnecessary waste of the area represented by the integral, and, therefore, in a reduction of the bandwidth. It is also clear that the limitation found by Bode applies to any impedance consisting of a reactive two-terminal-pair network terminated in a parallel

RC combination. In this case, however, it is to be expected that additional, and possibly more stringent, limitations would be imposed by the reactive network. These additional limitations were not investigated by Bode.

The above discussion indicates the existence of definite limitations on the broadband matching of any given load impedance. These limitations must originate from some conditions of physical realizability of the function  $\rho$  representing the input reflection coefficient, conditions which must, in their turn, depend on the load impedance. For the purpose of discussion, one can then divide the matching problem in three parts as follows.

- Given an impedance function  $Z_L$ , subject only to the restriction of being realizable by means of a finite number of lumped elements, find the conditions of physical realizability for the reflection-coefficient function  $\rho$  of a reactive two-terminal-pair network terminated in  $Z_L$ .

- From the conditions of physical realizability for  $\rho$ , determine the minimum tolerance on the magnitude of the reflection coefficient over a prescribed frequency band.

- Obtain appropriate functions for  $\rho$  which satisfy the conditions of physical realizability and, at the same time, lead to a matching network requiring a finite number of elements.

## 2. Physical Realizability

Darlington has shown<sup>3</sup> that any physically realizable impedance function can be considered as the input impedance of a reactive two-terminal-pair network terminated in a pure resistance. This resistance can be made equal to one ohm in all cases by incorporating an appropriate ideal transformer in the reactive network. The network shown in Fig. 1 can then be transformed as indicated in Fig. 2.

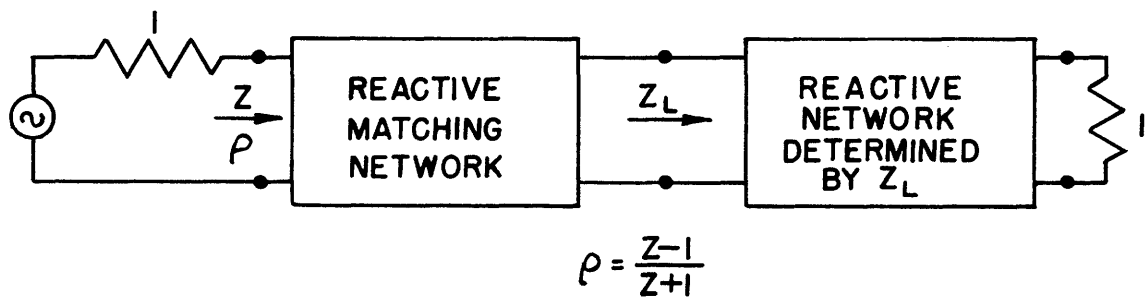


Figure 2. Matching of an arbitrary load impedance.

At this point the problem under consideration takes a form particularly interesting from a general network-theory point of view. It can be shown that the over-all characteristics of a two-terminal-pair reactive network are completely specified, apart from an all-pass network in cascade, by the input impedance (or the reflection coefficient) measured at one pair of terminals when a one-ohm resistance is connected to the other pair of terminals. It follows that the conditions of physical realizability for  $\rho$  (see Fig. 2) are the same as the conditions that must be satisfied by any other function or set of functions representing the over-all characteristics of the two reactive networks of Fig. 2 in cascade. In conclusion the problem can be restated as follows:

Given two reactive two-terminal-pair networks of which one is fixed, the other arbitrary, determine the conditions of physical realizability for the over-all characteristics of the two networks connected in cascade.

In studying this problem it is convenient to turn the network of Fig. 2 end to end, as indicated in Fig. 3, so that the network resulting from the Darlington representation of the load impedance becomes the network  $N'$ , and the matching network to be determined becomes  $N''$ . The reflection coefficients  $\rho_1$  and  $\rho_2$  refer to the whole network  $N$  terminated on both sides in one-ohm resistances. The transmission coefficient  $t$  of  $N$

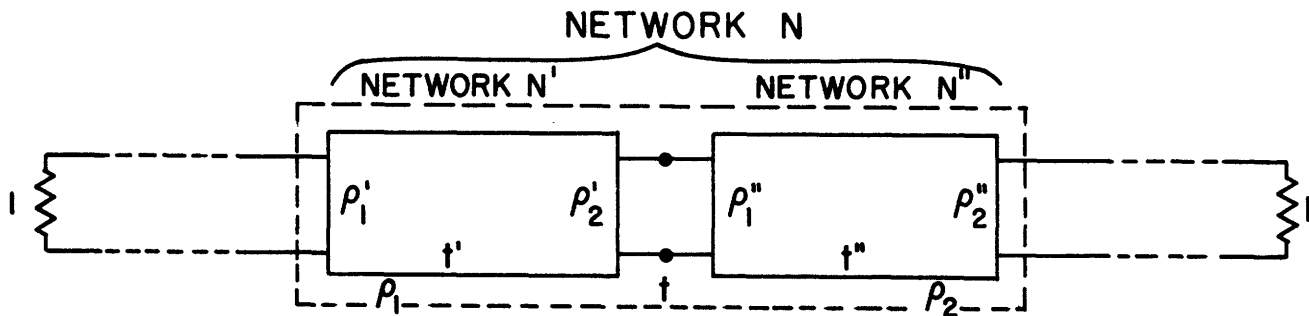


Figure 3. Two reactive networks in cascade.

is defined as the ratio of the voltage of the transmitted wave to the voltage of the incident wave with one-ohm terminations. The primed and double-primed symbols refer to the networks  $N'$  and  $N''$  respectively, and represent the reflection and transmission coefficients of these two networks when they are separately terminated in one-ohm resistances. These coefficients are functions of the real frequency  $\omega$ , and more precisely, are analytic functions of the complex frequency variable  $\lambda = \sigma + j\omega$ . The functional properties of the  $\rho$ 's and the  $t$ 's and the relations between them are summarized in Appendix I.

In considering the physical realizability problem, the first question that one is likely to ask is: Are there any characteristics of  $N'$  which must belong also to the whole network  $N$ , irrespective of  $N''$ ? A partial answer to this question is suggested immediately by the physical structure of the system. If  $t'$  is zero at a real frequency, that is, at any point of the imaginary axis of the  $\lambda$ -plane, then a wave of that frequency traveling from left to right would be completely stopped by  $N'$ , so that no part of the wave would come out of  $N''$  or even enter it. It follows that any point of the imaginary axis which is a zero of the transmission coefficient  $t'$  must necessarily be a zero of transmission for the whole network  $N$ , and, therefore, must be a zero of  $t$ . Furthermore, the reflected wave at the input terminals cannot depend on  $N''$  if no part of the incident wave reaches  $N''$ . Therefore,  $\rho_1$  must be equal to  $\rho_1'$  for any value of  $\lambda=j\omega$  for which  $t'$  is zero.

It is clear at this point that one should investigate carefully the effects on  $\rho_1$  and  $t$  of the presence in  $t'$  of a zero of arbitrary multiplicity located at any point of the complex  $\lambda$ -plane. The starting point for such an investigation is provided by the two equations

$$t = \frac{t' t''}{1 - \rho_2' \rho_1''}, \quad (5)$$

$$\rho_1 = \rho_1' + \rho_1'' \frac{(t')^2}{1 - \rho_2' \rho_1''}. \quad (6)$$

It is clear that all the zeros of  $t'$  are also zeros of  $t$  with at least the same multiplicity, provided the denominator of Eq. (5) is finite. It can be shown, on the other hand, that this denominator cannot vanish in the right half of the  $\lambda$ -plane, and that if it has a zero on the imaginary axis, this zero must have multiplicity equal to one and must coincide with a zero of  $t''$ . On the contrary, the zeros of  $t'$  in the left half of the  $\lambda$ -plane may not be present in  $t$  because the factor in the denominator can have zeros of arbitrary multiplicity in that part of the plane. It must be noted, however, in this regard, that if  $t'$  has a zero in the left half-plane, it must also have a zero symmetrically located in the right half-plane (see Appendix I), which must be present in  $t$ . Therefore the elimination of a zero in the left half-plane is, in a certain sense, only apparent. In conclusion, if  $t'$  has a zero in the right half-plane or on the imaginary axis,  $t$  must have the same zero with at least the same multiplicity.

With regard to the behavior of the reflection coefficient  $\rho_1$  at any point in the right half-plane or on the imaginary axis, at which  $t$  has a zero of multiplicity  $n$ , Eq. (6) indicates that  $\rho_1$  and its first  $2n-1$

derivatives are equal, respectively, to  $\rho_1^0$  and its corresponding derivatives, and therefore are independent of the network  $N''$ . The special case of a zero of  $t$  at a point of the imaginary axis at which the denominator of Eq. (6) vanishes will be discussed later.

For reasons that will become clear later, it is more convenient to consider the behavior of the function  $\ln 1/\rho_1$  instead of the reflection coefficient itself. On the other hand, if  $\rho_1$  and its first  $2n-1$  derivatives are independent of  $N''$ , the corresponding value and derivatives of  $\ln 1/\rho_1$  are also independent of  $N''$ . It follows that the first  $2n$  coefficients of the Taylor series for  $\ln 1/\rho_1$  about a zero of  $t'$  of multiplicity  $n$  in the right half-plane or on the imaginary axis will be independent of  $N''$ . In addition these coefficients are simply related to the locations of the zeros and poles of  $\rho_1$ , as indicated below.

In the particular case of a zero of  $t'$  at the origin, one has

$$\ln \frac{1}{\rho_1} = j\beta + A_1^0 \lambda + A_3^0 \lambda^3 + \dots + A_{2n-3}^0 \lambda^{2n-3} + A_{2n-1}^0 \lambda^{2n-1} + \dots \quad (7)$$

where  $\beta$  is equal to zero or  $\pi$ , depending on the sign of  $\rho_1$ . The coefficients of this series are all real because on the imaginary axis the magnitude of  $\rho_1$  is an even function of  $\omega$  and the phase is an odd function of  $\omega$ . In addition the even coefficients up to and including  $A_{2(n-1)}^0$  vanish because of the zero of  $t$  of multiplicity  $n$  at the origin. The odd coefficients are given by

$$A_{2k+1}^0 = \frac{1}{2k+1} \left( \sum_i \lambda_{oi}^{-(2k+1)} - \sum_i \lambda_{pi}^{-(2k+1)} \right), \quad (8)$$

where the  $\lambda_{oi}$  and the  $\lambda_{pi}$  are, respectively, the zeros and the poles of  $\rho_1$ . For a zero of  $t'$  at infinity one obtains similarly

$$\ln \frac{1}{\rho_1} = j\beta + A_1^\infty \lambda^{-1} + A_3^\infty \lambda^{-3} + \dots + A_{2n-3}^\infty \lambda^{-(2n-3)} + A_{2n-1}^\infty \lambda^{-(2n-1)} + \dots, \quad (9)$$

where

$$A_{2k+1}^\infty = \frac{1}{2k+1} \left( \sum_i \lambda_{oi}^{2k+1} - \sum_i \lambda_{pi}^{2k+1} \right). \quad (10)$$

In the case of a zero of  $t'$  at a point  $\omega_v$  of the imaginary axis, the even coefficients are real and the odd coefficients are imaginary up to and including the order  $2n-1$ . One has then

$$\ln \frac{1}{\rho_1} = jB_0^{\omega_v} + A_1^{\omega_v}(\lambda - j\omega_v) + jB_2^{\omega_v}(\lambda - j\omega_v)^2 + A_3^{\omega_v}(\lambda - j\omega_v)^3 + \dots \quad (11)$$

$$+ jB_{2n-2}^{\omega_v}(\lambda - j\omega_v)^{2n-2} + A_{2n-1}^{\omega_v}(\lambda - j\omega_v)^{2n-1} + \dots$$

where

$$(\ln \frac{1}{\rho_1})_{\lambda=j\omega_v} = j B_0^{\omega_v}, \quad (12)$$

$$\frac{1}{k} \left[ \sum_i (\lambda_{oi} - j\omega_v)^{-k} - \sum_i (\lambda_{pi} - j\omega_v)^{-k} \right] = \begin{cases} j B_k^{\omega_v} & \text{for } k \text{ even } \leq 2n-2 \\ A_k^{\omega_v} & \text{for } k \text{ odd } \leq 2n-1. \end{cases} \quad (13)$$

It is, of course, understood that if  $t'$  has a zero at a point  $j\omega_v$ , it must also have a conjugate zero at  $-j\omega_v$ . The coefficients of the series about the point  $-j\omega_v$  are the conjugates of the coefficients of the series (11).

In considering the case of a zero of  $t'$  at a point  $\sigma_v$  of the positive real axis, one must remember that the reflection coefficient  $\rho_1$  may have a zero of multiplicity  $n_o$  at that point, in which case it must also have a pole of the same multiplicity at the symmetrical point  $-\sigma_v$ . Since the function  $\ln 1/\rho_1$  is then singular at the point  $\sigma_v$ , one considers in its place the function

$$\ln \left\{ \frac{1}{\rho_1} \left( \frac{\lambda - \sigma_v}{\lambda + \sigma_v} \right)^{n_o} \right\} \quad (14)$$

from which the two singularities have been removed. Following the same line of thought as in the case of  $\ln 1/\rho_1$ , one can show without difficulty that the value of the new function (14) and its first  $(2n-n_o-1)$  derivatives at the point  $\sigma_v$  are independent of  $N''$ . Using the Taylor series for this function,  $\ln 1/\rho_1$  can be written finally in the form

$$\begin{aligned} \ln \frac{1}{\rho_1} = n_o \ln \frac{\lambda + \sigma_v}{\lambda - \sigma_v} + A_0^{\sigma_v} + j\beta + A_1^{\sigma_v}(\lambda - \sigma_v) + A_2^{\sigma_v}(\lambda - \sigma_v)^2 + \dots \\ + A_{2n-n_o-2}^{\sigma_v}(\lambda - \sigma_v)^{2n-n_o-2} + A_{2n-n_o-1}^{\sigma_v}(\lambda - \sigma_v)^{2n-n_o-1} + \dots \end{aligned} \quad (15)$$

where

$$\ln \left[ \frac{1}{\rho_1} \left( \frac{\lambda - \sigma_v}{\lambda + \sigma_v} \right)^{n_o} \right]_{\lambda=\sigma_v} = A_o^{\sigma_v} + j\beta , \quad (16)$$

$$A_k^{\sigma_v} = \frac{1}{k} \left[ \sum_i (\lambda_{oi} - \sigma_v)^{-k} - \sum_i (\lambda_{pi} - \sigma_v)^{-k} \right]. \quad (17)$$

The zero at  $\sigma_v$  and the pole at  $-\sigma_v$  must, of course, be excluded from the above summations. The case of a zero of  $t'$  at an arbitrary point  $\lambda_v$  of the right half-plane is treated in the same manner. One obtains in this case

$$\begin{aligned} \ln \frac{1}{\rho_1} &= n_o \ln \frac{(\lambda - \lambda_v)(\lambda - \bar{\lambda}_v)}{(\lambda + \lambda_v)(\lambda + \bar{\lambda}_v)} + (A_o^{\lambda_v} + jB_o^{\lambda_v}) + (A_1^{\lambda_v} + jB_1^{\lambda_v})(\lambda - \lambda_v) + (A_2^{\lambda_v} + jB_2^{\lambda_v})(\lambda - \lambda_v)^2 + \\ &\dots + [A_{(2n-n_o-2)}^{\lambda_v} + jB_{(2n-n_o-2)}^{\lambda_v}] (\lambda - \lambda_v)^{2n-n_o-2} + [A_{(2n-n_o-1)}^{\lambda_v} + jB_{(2n-n_o-1)}^{\lambda_v}] (\lambda - \lambda_v)^{2n-n_o-1} + \dots \end{aligned} \quad (18)$$

where

$$A_o^{\lambda_v} + jB_o^{\lambda_v} = \ln \left\{ \frac{1}{\rho_1} \left[ \frac{(\lambda - \lambda_v)(\lambda - \bar{\lambda}_v)}{(\lambda + \lambda_v)(\lambda + \bar{\lambda}_v)} \right]^{n_o} \right\}_{\lambda=\lambda_v}, \quad (19)$$

$$A_k^{\lambda_v} + jB_k^{\lambda_v} = \frac{1}{k} \left[ \sum_i (\lambda_{oi} - \lambda_v)^{-k} - \sum_i (\lambda_{pi} - \lambda_v)^{-k} \right]. \quad (20)$$

Also in this case the pair of zeros at  $\lambda_v$  and  $\bar{\lambda}_v$  and the pair of poles at  $-\lambda_v$  and  $-\bar{\lambda}_v$  must be excluded from the above summations. The coefficients of the series about the zero of  $t'$  at  $\bar{\lambda}_v$  are the conjugates of the coefficients of the series (18).

The coefficients of the series (7), (9), (11), (15), and (18) up to the order  $2n-n_o-1$  included are completely fixed by the given network  $N'$ , with the possible exception of the last coefficients, of order  $2n-1$ , in the case of a zero of  $t'$  on the imaginary axis. Such an exception arises from the fact that the factor  $1 - \rho_2! \rho_1^n$ , in Eqs. (5) and (6) may have a zero of multiplicity one coinciding with a zero of  $t'$  on the imaginary axis. This situation leads to what may be called a degenerate case, because  $t''$  must have then a zero at the same point which effectively combines with the zero of  $t'$ . In fact, the resulting multiplicity of the zero of the over-all

transmission coefficient  $t$  is, in this case, one less than the sum of the multiplicities of the zeros of  $t'$  and  $t''$  at the same point, as indicated by Eq. (5). The impedances measured at the common terminals of  $N'$  and  $N''$  in the two directions at this frequency must be pure reactances with equal magnitudes and opposite signs.

Two simple examples of degenerate zeros are shown in Fig. 4 for the case of a zero at infinity (a), and a zero at  $\lambda = +j\omega_v$ , (b). It is clear in these examples that the zeros of transmission of  $N'$  and  $N''$  will combine in such a way that the  $(2n-1)^{th}$  derivative of  $\rho_1$  will depend on  $N''$  as well as on  $N'$  and therefore will not be equal to the corresponding derivatives of  $\rho_1$ .

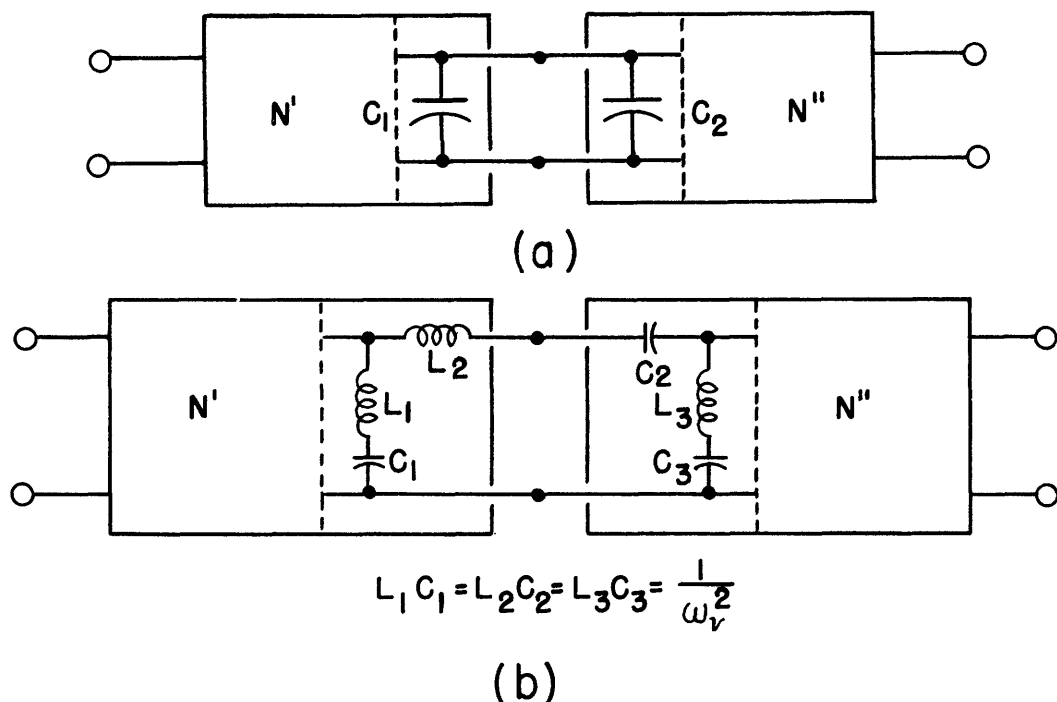


Figure 4. Two examples of degenerate zeros of transmission.

Equation (6) shows that this is true in the general case of a degenerate zero of transmission. The examples of Fig. 4 indicate, however, that the change of the behavior of the input reflection coefficient when  $N''$  is connected to  $N'$  must take place in a particular direction. For instance, in the case of Fig. 4a, the fact that the total shunt capacitance  $C_1 + C_2$  is larger than the capacitance in  $N'$  alone must somehow restrict the possible change of behavior. It can be shown\* that, in the case of a zero of  $t'$  of multiplicity  $n$  on the imaginary axis, the coefficient  $A_{2n-1}$  of the Taylor

---

\* For a proof of this and other similar statements, see the original Doctorate Thesis, available in the Library of the Massachusetts Institute of Technology.

series is always increased by the presence of  $N''$  when  $n$  is odd, and is always decreased when  $n$  is even. The physical significance of this restriction and its practical importance will become clearer in the next section.

The analysis carried out above has led to the formulation of a number of necessary conditions that must be satisfied by the functions representing the network  $N$  in order to be physically realizable by means of the given network  $N'$  and the arbitrary network  $N''$  connected in cascade. These necessary conditions are summarized below for convenience. With reference to Fig. 3, all the zeros of  $t'$  which lie in the right half-plane or on the imaginary axis must appear as zeros of  $t$  with at least the same multiplicity. Moreover, a certain number of coefficients of the Taylor series for  $\ln 1/\rho_1$  about each of the zeros of transmission must be equal to the corresponding coefficients for  $\ln 1/\rho'_1$  or, in other words, must be independent of  $N''$ . The resulting number of real quantities independent of  $N''$  is equal to the multiplicity of the corresponding zero of transmission in the case of a zero located at the origin or at infinity, to twice the multiplicity in the case of a pair of zeros on either the real or the imaginary axis, to four times the multiplicity in the case of a quadruplet of complex zeros. If a pair of zeros of  $t'$  at  $-\lambda_v$  and  $-\bar{\lambda}_v$  in the left half-plane is partially or totally eliminated by a pair of poles of  $t'$  of multiplicity  $n_o$  located at the same points, a number  $2n_o$  of these real quantities independent of  $N''$  are missing. In this case, however, an equivalent number of conditions are imposed by the fact that  $\rho_1$  must have a pair of poles of multiplicity  $n_o$  at  $-\lambda_v$  and  $-\bar{\lambda}_v$  and, therefore, a pair of zeros with the same multiplicity at  $\lambda_v$  and  $\bar{\lambda}_v$  (see Appendix I). A similar situation arises in the case of the elimination of a zero of transmission at  $-\sigma_v$  on the real axis. The case of a degenerate zero on the imaginary axis does not lead to any special difficulty.

Darlington has shown<sup>3</sup> that any two-terminal-pair reactive network can be constructed as a chain of sections each representing a simple zero of transmission, a pair of zeros, or a quadruplet of zeros; zeros of multiplicity  $n$  are represented by  $n$  similar sections. The order in which the sections are connected is immaterial, as far as the physical realizability of the network is concerned. Each section involves a number of elements equal to the number of zeros represented by the section plus the number of real quantities necessary to specify the location of the zeros. The resulting network is shown to require a minimum number of elements.

It is clear at this point that the number of necessary conditions imposed on  $\rho_1$  and  $t$  by  $N'$  is equal to the number of independent parameters by which  $N'$  is completely specified. On the other hand, the conditions imposed by  $N'$  are independent of one another; it can be shown, in fact, by interchanging the sections forming  $N'$  that any one of these conditions can be changed without disturbing the others. To prove that

these conditions of physical realizability are sufficient as well as necessary one needs only to observe, in addition, that the network  $N$  defined by  $\rho_1$  and  $t$  can be constructed in two parts, the first of which contains all the sections representing the zeros of  $t'$ . If the correct sign of  $\rho_1$  is used (the sign differentiates the desired network from its reciprocal), this first part with an appropriate ideal transformer at the output terminals, can be identified with the given network  $N'$ , because all the sections contained in it are completely specified by the conditions of physical realizability imposed on  $\rho_1$ , which, on the other hand, completely specify  $N'$ . The second part of the network is certainly realizable because it can be obtained by simply completing the synthesis procedure developed by Darlington.

The above analysis has led thus to the determination of necessary and sufficient conditions for the physical realizability of the reflection coefficient  $\rho_1$  when  $\rho_1^!$  and  $t'$  are specified. In a practical matching problem, however,  $\rho_1^!$  and  $t'$  are given indirectly through  $\rho_2^!$ , which, in turn, is specified by the load impedance  $Z_L$ . On the other hand,  $\rho_1^!$  and  $t'$  are completely specified by  $\rho_2^!$ , apart from an arbitrary all-pass network connected to terminals (1) of  $N'$ . This arbitrary network, however, can be neglected because it does not produce any reflection by itself nor does it change the phase of any other reflection when the network  $N'$  is driven from terminals 2. Therefore, for the purposes of this discussion,  $N'$  is completely specified by  $Z_L$ . On the other hand, one can observe that the reflection coefficient which is measured in an actual matching problem is not  $\rho_1$  but  $\rho_2$ , since the source is connected to terminals 2 of  $N$ . This fact, however, is immaterial since only the magnitude of  $\rho_2$  is of importance in most cases and  $|\rho_2| = |\rho_1|$  for  $\lambda=j\omega$ . Moreover, if one were interested in the whole function  $\rho_2$ , it would be a simple matter to express the conditions of physical realizability in terms of the zeros and poles of  $\rho_2$ , since they are simply related to the corresponding singularities of  $\rho_1$  (see Appendix I).

### 3. Limitations on the Tolerance and the Bandwidth

The next step in the solution of the matching problem is the transformation of the conditions of physical realizability derived above into a set of relations suitable for the determination of the theoretical limitations on the bandwidth and tolerance of match. Such relations must involve the behavior of the magnitude of the reflection coefficient on the imaginary axis, that is at real frequencies, and the coefficients of the Taylor series which are fixed by the given load impedance.

Cauchy's integral relations provide the appropriate tool for the desired transformation. The function  $\ln 1/\rho$  is multiplied first by a

function having poles of appropriate multiplicity at the zero, pair, or quadruplet of zeros of  $t'$  under consideration and is integrated then over the contour formed by the imaginary axis and the semicircle at infinity in the right half-plane; appropriate indentations must be provided when the poles are located on the imaginary axis. If  $\rho_1$  has zeros in the right half-plane, it is more convenient to use instead of  $\rho_1$  the function  $\rho_0$  obtained from  $\rho_1$  by moving all the zeros in the right half-plane to symmetrical positions in the left half-plane. This new function  $\rho_0$  has the same magnitude as  $\rho_1$  on the imaginary axis. It is also convenient to make  $\rho_0$  positive at the origin by changing its sign if necessary. The coefficients  $F$  and  $G$  of the Taylor series for  $\ln 1/\rho_0$  corresponding to the  $A$ 's and  $B$ 's for  $\ln 1/\rho_1$  are given in Table II. The integral relations obtained by following this procedure are collected in Table I and the weighting functions  $f$  and  $g$ , which are part of the integrand are tabulated in Table III. The  $\lambda_{r_1}$  appearing in Table II are the zeros of  $\rho_1$  that lie in the right half-plane.

TABLE I. Integral Relations Obtained from the Conditions of Physical Realizability

Zero of $t'$	Frequency variable	Integral relation
origin	$\omega$	$\int_0^\infty \omega^{-2(k+1)} \ln(1/ \rho_1 ) d\omega = (-1)^k \frac{\pi}{2} F_{2k+1}^0$
infinity	$\omega$	$\int_0^\infty \omega^{2k} \ln(1/ \rho_1 ) d\omega = (-1)^k \frac{\pi}{2} F_{2k+1}^\infty$
$\pm j\omega_v$	$x = \omega/\omega_v$	$\int_0^\infty g_{2k}^{\omega_v} \ln(1/ \rho_1 ) dx = (-1)^{k+1} \frac{\pi}{2} \omega_v^{2k} G_{2k}^{\omega_v}$
"	"	$\int_0^\infty f_{2k+1}^{\omega_v} \ln(1/ \rho_1 ) dx = (-1)^k \frac{\pi}{2} \omega_v^{2k+1} F_{2k+1}^{\omega_v}$
$\pm \sigma_v$	$x = \omega/\sigma_v$	$\int_0^\infty f_k^{\sigma_v} \ln(1/ \rho_1 ) dx = (-1)^k \frac{\pi}{2} \sigma_v^k F_k^{\sigma_v}$
$\pm \sigma_v + j\omega_v$	$x = \omega/ \lambda_v $	$\int_0^\infty f_{2k}^{\lambda_v} \ln(1/ \rho_1 ) dx = (-1)^k \frac{\pi}{2}  \lambda_v ^{2k} F_{2k}^{\lambda_v}$
"	"	$\int_0^\infty g_{2k}^{\lambda_v} \ln(1/ \rho_1 ) dx = (-1)^{k+1} \frac{\pi}{2}  \lambda_v ^{2k} G_{2k}^{\lambda_v}$
"	"	$\int_0^\infty f_{2k+1}^{\lambda_v} \ln(1/ \rho_1 ) dx = (-1)^k \frac{\pi}{2}  \lambda_v ^{2k+1} F_{2k+1}^{\lambda_v}$
"	"	$\int_0^\infty g_{2k+1}^{\lambda_v} \ln(1/ \rho_1 ) dx = (-1)^k \frac{\pi}{2}  \lambda_v ^{2k+1} G_{2k+1}^{\lambda_v}$

Table II. The Coefficients Appearing in the Integral Relations of Table I.

$F_{2k+1}^0 = A_{2k+1}^0 - \frac{2}{2k+1} \sum_i \lambda_{ri}^{-(2k+1)}$
$F_{2k+1}^\infty = A_{2k+1}^\infty - \frac{2}{2k+1} \sum_i \lambda_{ri}^{2k+1}$
$G_o^{\omega_v} = B_o^{\omega_v} + j \left[ \sum_i \ln \frac{-\bar{\lambda}_{ri} - j\omega_v}{\lambda_{ri} - j\omega_v} \right] + \beta$
$F_{2k+1}^{\omega_v} = A_{2k+1}^{\omega_v} - \frac{2}{2k+1} \operatorname{Re} \sum_i (\lambda_{ri} - j\omega_v)^{-2k+1}$
$G_{2k}^{\omega_v} = B_{2k}^{\omega_v} - \frac{1}{k} \operatorname{Im} \sum_i (\lambda_{ri} - j\omega_v)^{-2k}$
$F_o^{\sigma_v} = A_o^{\sigma_v} - \operatorname{Re} \sum_i \frac{-\bar{\lambda}_{ri} - \sigma_v}{\lambda_{ri} - \sigma_v}$
$F_k^{\sigma_v} = A_k^{\sigma_v} - \frac{1}{k} \left[ \sum_i (\lambda_{ri} - \sigma_v)^{-k} - \sum_i (-\bar{\lambda}_{ri} - \sigma_v)^{-k} \right]$
$F_o^{\lambda_v} + jG_o^{\lambda_v} = A_o^{\lambda_v} + jB_o^{\lambda_v} - \sum_i \ln \frac{-\bar{\lambda}_{ri} - \lambda_v}{\lambda_{ri} - \lambda_v} + j\beta$
$F_k^{\lambda_v} + jG_k^{\lambda_v} = A_k^{\lambda_v} + jB_k^{\lambda_v} - \frac{1}{k} \left[ \sum_i (\lambda_{ri} - \lambda_v)^{-k} - \sum_i (-\bar{\lambda}_{ri} - \lambda_v)^{-k} \right]$
$\beta = \begin{cases} 0 & \text{if } \rho_1(0) \text{ and } \rho_o(0) \text{ have the same sign} \\ \pi & \text{if } \rho_1(0) \text{ and } \rho_o(0) \text{ have opposite signs} \end{cases}$

Table III. The Functions Appearing in the Integral Relations of Table I.

$f_{2k+1}^{\omega_v} = \frac{(1+x)^{2(k+1)} + (1-x)^{2(k+1)}}{2(1-x^2)^{2(k+1)}}$
$g_{2k}^{\omega_v} = \frac{(1+x)^{2k+1} + (1-x)^{2k+1}}{2(1-x^2)^{2k+1}}$
$f_k^{\sigma_v} = \frac{(1+jx)^{k+1} + (1-jx)^{k+1}}{2(1+x^2)^{k+1}}$
$f_{2k}^{\lambda_v} = (-1)^k \left[ \left\{ \left[ \delta + j(x + \sqrt{1-\delta^2}) \right]^{-(2k+1)} - \left[ -\delta + j(x - \sqrt{1-\delta^2}) \right]^{-(2k+1)} \right\} + \left\{ \begin{array}{l} + \\ - \end{array} \right\} \left\{ \left[ \delta + j(x - \sqrt{1-\delta^2}) \right]^{-(2k+1)} - \left[ -\delta + j(x + \sqrt{1-\delta^2}) \right]^{-(2k+1)} \right\} \right]$
$g_{2k}^{\lambda_v} = (-1)^{k+1} \left[ (-1)^k \left[ \left\{ \left[ \delta + j(x + \sqrt{1-\delta^2}) \right]^{-2(k+1)} + \left[ -\delta + j(x - \sqrt{1-\delta^2}) \right]^{-2(k+1)} \right\} + \left\{ \begin{array}{l} + \\ - \end{array} \right\} \left\{ \left[ \delta + j(x - \sqrt{1-\delta^2}) \right]^{-2(k+1)} + \left[ -\delta + j(x + \sqrt{1-\delta^2}) \right]^{-2(k+1)} \right\} \right] \right]$
$f_{2k+1}^{\lambda_v} = \left[ (-1)^k \left[ \left\{ \left[ \delta + j(x + \sqrt{1-\delta^2}) \right]^{-2(k+1)} + \left[ -\delta + j(x - \sqrt{1-\delta^2}) \right]^{-2(k+1)} \right\} + \left\{ \begin{array}{l} + \\ - \end{array} \right\} \left\{ \left[ \delta + j(x - \sqrt{1-\delta^2}) \right]^{-2(k+1)} + \left[ -\delta + j(x + \sqrt{1-\delta^2}) \right]^{-2(k+1)} \right\} \right] \right]$
$\delta = \frac{\sigma_v}{ \lambda_v }$

The integral relations of Table I are the crux of the paper because they express the conditions of physical realizability in terms of the observable behavior of a physical quantity, namely the behavior, over the frequency spectrum, of the magnitude of the reflection coefficient. To obtain the optimum tolerance of match, one must determine then the function  $|p_1|$  which is a solution of the set of equations formed by these integral relations and whose maximum deviation from zero over a prescribed frequency band is a minimum. This problem was solved only in very special cases; however, the relations of Table I yield directly useful information on the nature of the theoretical limitations on the tolerance and bandwidth of match, as indicated below.

The special case of a network  $N'$  having all the zeros of transmission at infinity will be considered first. Such a network can be realized in either the form of a low-pass ladder structure of the type shown in Fig. 5, or in the dual form (starting with a shunt capacitance).

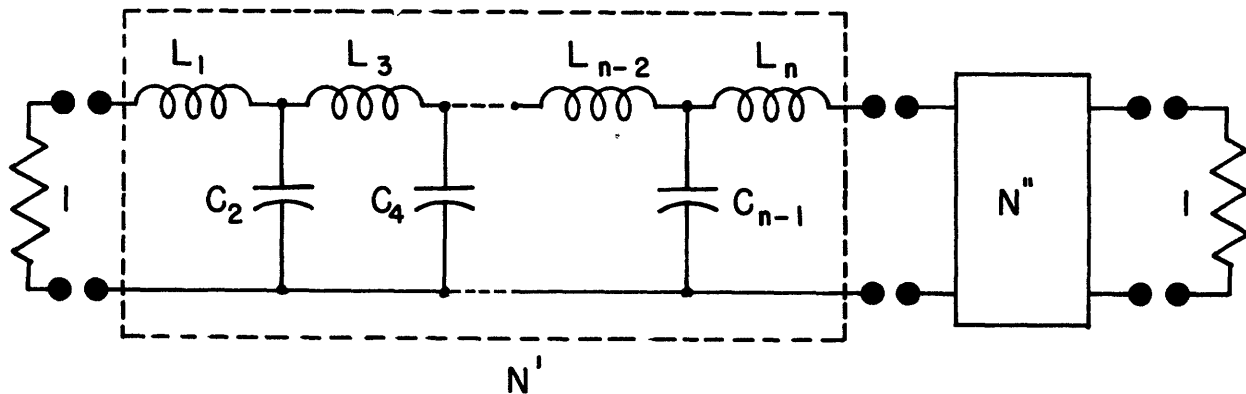


Figure 5. Network  $N'$  with  $n$  zeros of transmission at infinity, and matching network  $N''$ .

In this former case the coefficient  $A_1$  depends on  $L_1$  alone,  $A_3$  depends on  $L_1$  and  $C_2$ ,  $A_5$  depends on  $L_1, C_2$ , and  $L_3$ , and so forth, since each of the elements represents a zero of transmission at infinity. The integral relations which apply to the case of a zero of transmission at infinity of multiplicity equal to 3 are rewritten below for convenience.

$$\int_0^\infty \ln \frac{1}{|p_1|} d\omega = \frac{\pi}{2} (A_1^\infty - 2 \sum_i \lambda_{r1}) \quad (21)$$

$$\int_0^\infty \omega^2 \ln \frac{1}{|p_1|} d\omega = -\frac{\pi}{2} (A_3^\infty - \frac{2}{3} \sum_i \lambda_{r1}^3) \quad (22)$$

$$\int_0^\infty \omega^4 \ln \frac{1}{|p_1|} d\omega = \frac{\pi}{2} (A_5^\infty - \frac{2}{5} \sum_i \lambda_{r1}^5) \quad (23)$$

The  $\lambda_{r1}$  are the zeros of  $p_1$  that lie in the right half-plane.

The left-hand side of the first equation represents the area under the curve  $\ln 1/|\rho_1|$  versus frequency. The coefficient  $A_1^\infty$  is fixed by the first element  $L_1$  of the network  $N'$ , while the  $\lambda_{ri}$  are arbitrary quantities subject only to two restrictions; namely, that their real parts must be positive and that they must appear in conjugate pairs if they are complex. It follows that the summation in Eq. (21) is always real and positive so that  $A_1^\infty$  sets an upper limit to the area represented by the integral. It is clear that the best possible utilization of this area is obtained when  $\ln 1/|\rho_1|$  is kept constant over the desired frequency band and is made equal to zero over the rest of the frequency spectrum. This situation is illustrated for the low-pass case in Fig. 6. If  $w$  is the desired

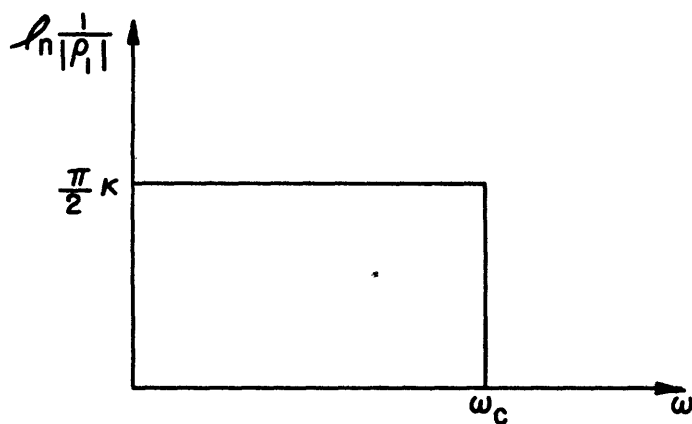


Figure 6. Optimum frequency response.

bandwidth ( $w = \omega_c$  in Fig. 6) the best possible tolerance is given by

$$\left[ \ln \frac{1}{|\rho_1|} \right]_{\max} = \frac{\pi}{2w} A_1^\infty . \quad (24)$$

This theoretical limitation was first found by Bode, as pointed out above. In fact, when the load consists of a parallel RC combination, the coefficient  $A_1^\infty$  becomes equal to  $2/RC$ . Bode, however, did not consider the case of a network  $N'$  consisting of more than one element. In this case a number of equations equal to the number of elements in  $N'$  will have to be satisfied simultaneously. Suppose, for instance, that  $N'$  contains two elements,  $L_1$  and  $C_2$ ; that is,  $N'$  has a zero of transmission of multiplicity equal to two, so that Eqs. (21) and (22) must be satisfied simultaneously. If the rectangular function which yields the optimum tolerance according to Eq. (24) is used in Eq. (22), the value of the integral may be larger or smaller than  $-\pi A_3^\infty/2$  ( $A_3^\infty$  is in general negative). If it is smaller, it is a simple matter to reduce the magnitude of the right-hand side of Eq. (22).

In fact, it was pointed out before that in the case of a degenerate zero of transmission, the algebraic value of  $A_3^\infty$  can be increased; that is, its absolute value can be decreased. Physically this operation amounts to starting the matching network  $N'$  with a shunt capacitance which has the effect of increasing the value of the capacitance  $C_2$  in  $N'$ . If on the contrary the value of the integral in Eq. (22) is larger than  $-\pi A_3^\infty/2$ , the optimum tolerance given by Eq. (24) cannot be reached. One observes then that the value of the summation in Eq. (22) can be either positive or negative, so that the value of the right-hand side of Eq. (22) can be increased by introducing appropriate zeros of  $\rho_1$  in the right half of the plane. These zeros, however, reduce necessarily the value of the right-hand side of Eq. (21), so that the area represented by the integral of Eq. (22) is increased at the expense of the area represented by the integral of Eq. (21).

With reference to Fig. 6, as an example, let the maximum value of  $\ln 1/|\rho_1|$  be equal to  $\pi K/2$ . One obtains from Eqs. (21) and (22) that

$$\omega_c^K = A_1^\infty - 2 \sum_i \lambda_{ri} , \quad (25)$$

$$\omega_c^{3K} = -3 A_3^\infty + 2 \sum_i \lambda_{ri}^3 . \quad (26)$$

The  $\lambda_{ri}$  must be selected so as to maximize the value of  $K$  for given values of  $\omega_c$ ,  $A_1^\infty$ , and  $A_3^\infty$ . It will be observed, first of all, that  $\rho_1$  can be multiplied by any factor of the type  $(\lambda - \lambda_r)/(\lambda + \lambda_r)$  without changing the value of  $\ln 1/|\rho_1|$  on the imaginary axis, so that the behavior of the magnitude of the reflection coefficient and the values of the  $\lambda_{ri}$  can be controlled independently. One observes next that since the summation in Eq. (22) must be made positive, both equations can be satisfied by using a single zero  $\lambda_r = \sigma_r$  located on the positive real axis. On the other hand, maximizing  $K$  is equivalent to making  $\sum_i \lambda_{ri}^3$  as large as possible while keeping  $\sum_i \lambda_{ri}$  as small as possible. Moreover, if  $\operatorname{Re} \lambda_{ri}^3 > 0$ , then  $\operatorname{Re} \lambda_{ri}^3 \leq \sigma_{ri}^3$ , and  $\sum_i \operatorname{Re} \lambda_{ri}^3 \leq (\sum_i \sigma_{ri})^3$ . It follows that the maximum value of  $K$  is obtained by using a single zero located at  $\sigma_r$ . Equations (25) and (26) then become

$$\omega_c^K = A_1^\infty - 2 \sigma_r , \quad (27)$$

$$\omega_c^{3K} = -3 A_3^\infty + 2 \sigma_r^3 . \quad (28)$$

Solving these two equations by eliminating  $\sigma_r$  yields the maximum theoretical value of  $K$  as a function of the cut-off frequency  $\omega_c$ . The maximum pass-band

value of  $\ln 1/|\rho_1|$  is plotted in Fig. 7 as a function of  $\omega_c/A_1^\infty$  for different values of the parameter  $-A_3^\infty/(A_1^\infty)^3$ . The curve  $K = A_1^\infty/\omega_c$  forms the boundary of the region in which the optimum design is obtained by simply increasing the value of the second element.

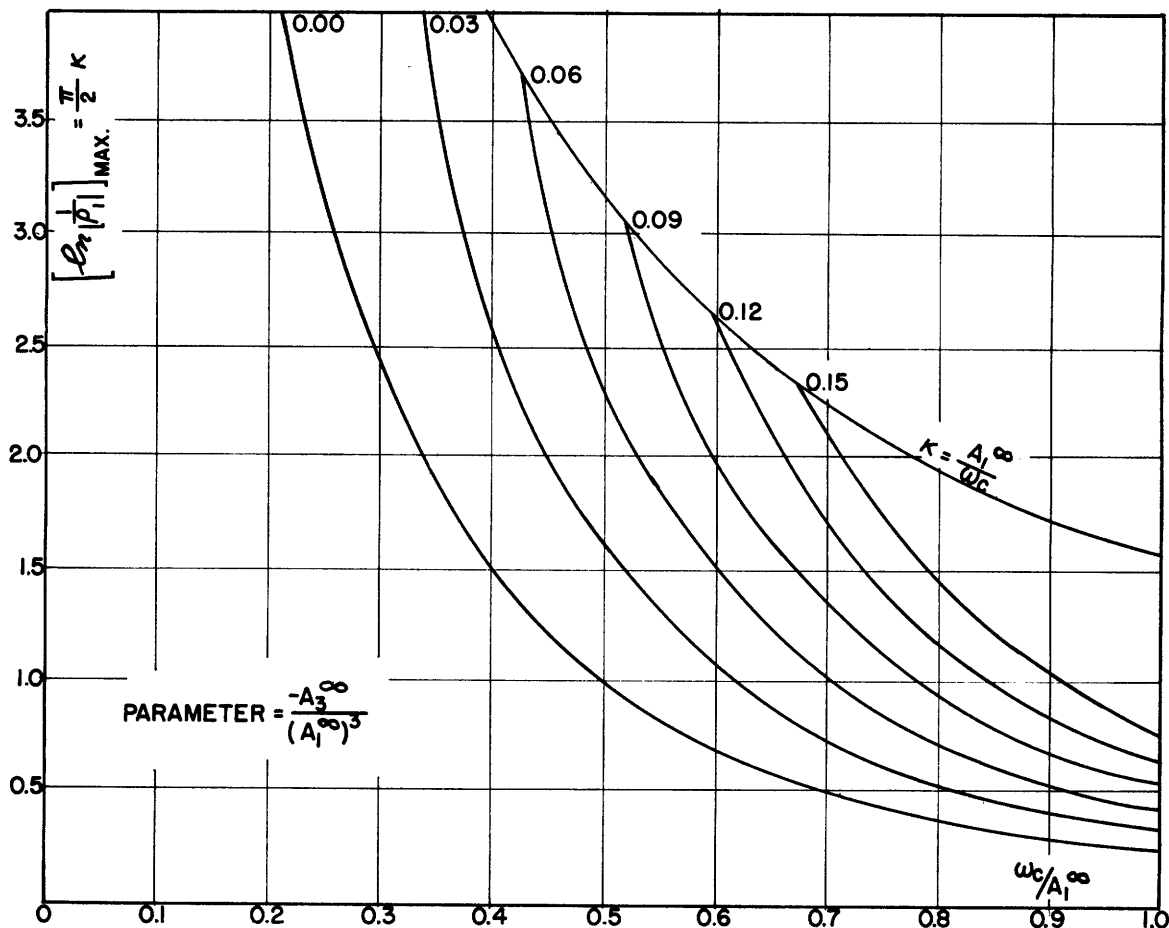


Figure 7. Optimum tolerance of match for a C-L-R impedance.

When the network  $N'$  consists of three or more elements, the problem of determining the optimum tolerance of match becomes much more difficult, and no general solution has been obtained. However, a few general considerations can be made. In the first place, the rectangular form of frequency behavior for  $\ln 1/|\rho_1|$  yields the optimum tolerance in all cases, because it provides the best utilization of the areas represented by the successive integrals. In the case of a passband extending from zero frequency to  $\omega_c$ , the equations to be satisfied take the general form

$$\omega_c^{2k+1} K = (-1)^k \left[ (2k+1) A_{2k+1}^{\infty} - 2 \sum_1 \lambda_{ri}^{2k+1} \right]. \quad (29)$$

In the last equation of the set  $k = n+1$ ,  $n$  being the number of elements in the network  $N'$ . It seems reasonable to expect that the number of  $\lambda_{ri}$  for which  $K$  is a maximum will be equal, in general, to the minimum number required for the solution of the set of equations. The reasoning followed in the case of two elements, however, could not be extended rigorously to the case of  $n$  elements. Moreover, the solution of such a system of equations might yield  $\lambda_{ri}$  with negative real parts which, of course, would not be acceptable. In this case more  $\lambda_{ri}$  would have to be used, and their values would have to be determined by maximizing  $K$ .

The coefficient  $A_{2n-1}$  in the last equation of any particular set can be changed, but only in one direction, by combining one zero of transmission of  $N'$  with a similar zero of transmission of  $N''$ , as pointed out above. It will be observed that the direction in which  $A_{2n-1}$  can be changed corresponds always to a decrease of the area represented by the integral on the right side of the same equation. It follows that one must determine first the optimum tolerance that can be obtained by neglecting the last element of the network  $N'$ , as was done in the case of two elements, to check whether the same tolerance could be obtained by simply increasing the value of this last element.

It is hardly necessary to point out that when the network  $N'$  contains three or more elements, the actual determination of the optimum tolerance requires the solution of a system of algebraic equations of fifth or higher degree. This difficulty cannot be avoided as long as the mathematical formulation of the problem remains the same. It is quite possible, however, that a different physical approach, such as, for instance, one based on the time response of the network rather than on the frequency response, might avoid this difficulty and be more successful.

The results obtained above can be applied directly to a number of networks derivable from the low-pass ladder structure by means of appropriate transformations of the frequency variables <sup>7,8</sup>, notably the

high-pass and the band-pass ladder structures. The high-pass structure has all its zeros of transmission at the origin, and can be obtained from the low-pass structure by interchanging inductances and condensers. The band-pass structure has zeros of transmission in equal number at the origin and at infinity; it can be obtained from the low-pass structure by tuning to the mean frequency every inductance with a series condenser, and every capacitance with a shunt inductance. When such a procedure is followed, the resulting pass band is numerically equal to the cut-off frequency of the original low-pass structure.

An additional remark is in order with regard to networks with zeros of transmission at both the origin and infinity. If the multiplicity of the zero at the origin is  $n_0$  and the multiplicity of the zero at infinity is  $n_\infty$ , the conditions of physical realizability for the matching network will yield  $n_0 + n_\infty$  equations of the types indicated in Table I. When a rectangular-shaped function is used for  $\ln 1/|\rho_1|$ , these equations take the forms

$$(\omega_2^{2k+1} - \omega_1^{2k+1}) K = (-1)^k \left[ (2k+1) A_{2k+1}^\infty - 2 \sum_i \lambda_{ri}^{2k+1} \right], \quad (30)$$

$$(\omega_1^{-(2k+1)} - \omega_2^{-(2k+1)}) K = (-1)^k \left[ (2k+1) A_{2k+1}^0 - 2 \sum_i \lambda_{ri}^{-(2k+1)} \right], \quad (31)$$

where  $\omega_1$  and  $\omega_2$  are, respectively, the low-frequency and the high-frequency ends of the pass band and  $K$  is the pass-band value of  $\ln 1/|\rho_1|$  divided by  $\pi/2$ . To determine the maximum value of  $K$ , one must solve simultaneously the whole set of equations. However, if  $\omega_2 \gg \omega_1$  the two sets of equations relating to the two zeros of transmission can be solved separately. In other words, the high-frequency response of the network can be considered independently of the low-frequency response. The two sets of equations will yield different values of  $K$  for given  $\omega_1$  and  $\omega_2$ , the smaller of which will represent the optimum tolerance of match.

The integral relations of Table I all have the same general form, irrespective of the location of the zero of transmission to which they refer. The integrand on the left-hand side consists of the function  $\ln 1/|\rho_1|$  multiplied by a weighting function which depends on the location of the zero of transmission. The right-hand side consists of the difference between a coefficient specified by the network  $N'$  and a summation involving the zeros of  $\rho_1$  that lie in the right half-plane and the location of the zero of transmission.

In the simple case concerning zeros of transmission at infinity and at the origin, the weighting functions are the even powers, positive and

negative respectively, of the frequency  $\omega$ . These functions have the effect of preventing the arbitrary distribution over the frequency spectrum of the area under the  $\ln 1/|\rho_1|$ -versus-frequency curve. In particular they prevent the value of  $\ln 1/|\rho_1|$  from remaining large when the frequency approaches infinity in the one case and zero in the other.

The weighting functions have similar properties in the case of a zero of transmission on the imaginary axis. In the first place the area represented by the integral in the equation involving  $A_1^{\omega\nu}$  can be equal, at most, to  $\pi A_0^{\omega\nu} w_{\nu}/2$  because the summation on the right-hand side of the equation is always positive. The corresponding weighting function  $f_1^{\omega\nu}$ , plotted in Fig. 8, has a sort of even symmetry with respect to the point  $\omega=w_{\nu}$ . This fact would indicate that the area represented by  $A_1^{\omega\nu}$  can be divided arbitrarily between the two sides of  $w_{\nu}$ . Such an arbitrary division, however, is not possible because the weighting function  $g_0^{\omega\nu}$  (plotted in Fig. 8) in the first equation of the set has a sort of odd symmetry with respect to the same point  $w_{\nu}$ . The division of the area is thus limited by the value of  $B_0^{\omega\nu}$  and by the fact that the use of any zero of  $\rho_1$  in the right half-plane to modify  $B_0^{\omega\nu}$  results in a decrease of the area represented by the integral in the equation involving  $A_1^{\omega\nu}$ . The weighting functions of higher order are, alternatively, of the even-symmetry and of the odd-symmetry types, and rise faster and faster with their order when  $\omega$  approaches  $w_{\nu}$ , as indicated in Fig. 8.

In the case of a zero of transmission on the real axis, the integral in the first equation can never be larger than  $\pi A_0^{\omega\nu}/2$  and, in addition, the integral in the second equation can never be smaller than  $(-\pi \sigma_{\nu} A_1^{\omega\nu}/2)$ . It will be noted in this regard that the weighting function  $f_0^{\omega\nu}$  is positive for all values of  $\omega$ , while the function  $f_1^{\omega\nu}$  is positive for  $\omega < \sigma_{\nu}$  and negative for  $\omega > \sigma_{\nu}$ , as shown in Fig. 9. It follows that, roughly speaking, the value of  $\ln 1/|\rho_1|$  is limited at low frequencies by the first equation and at high frequencies by the second equation. If the multiplicity of the zero of transmission is larger than one, the areas represented by the integrals in these first two equations are prevented from being distributed arbitrarily over the frequency spectrum by equations of higher order. The first six weighting functions corresponding to a zero of transmission of multiplicity equal to three are plotted in Fig. 9.

In the case of zeros of transmission at complex frequencies, the weighting functions  $f_k$  and  $g_k$  lead to limitations very similar to the ones discussed above for the cases of zeros of transmission on the real and on the imaginary axis. They reduce actually to the corresponding functions for these cases when the parameter  $\delta = \sigma_{\nu}/|\lambda_{\nu}|$  approaches infinity and zero, respectively. The weighting functions of orders 0, 1, and 2 are plotted in Figs. 10 to 15 for  $\delta$  equal to 0.5 and 0.05.

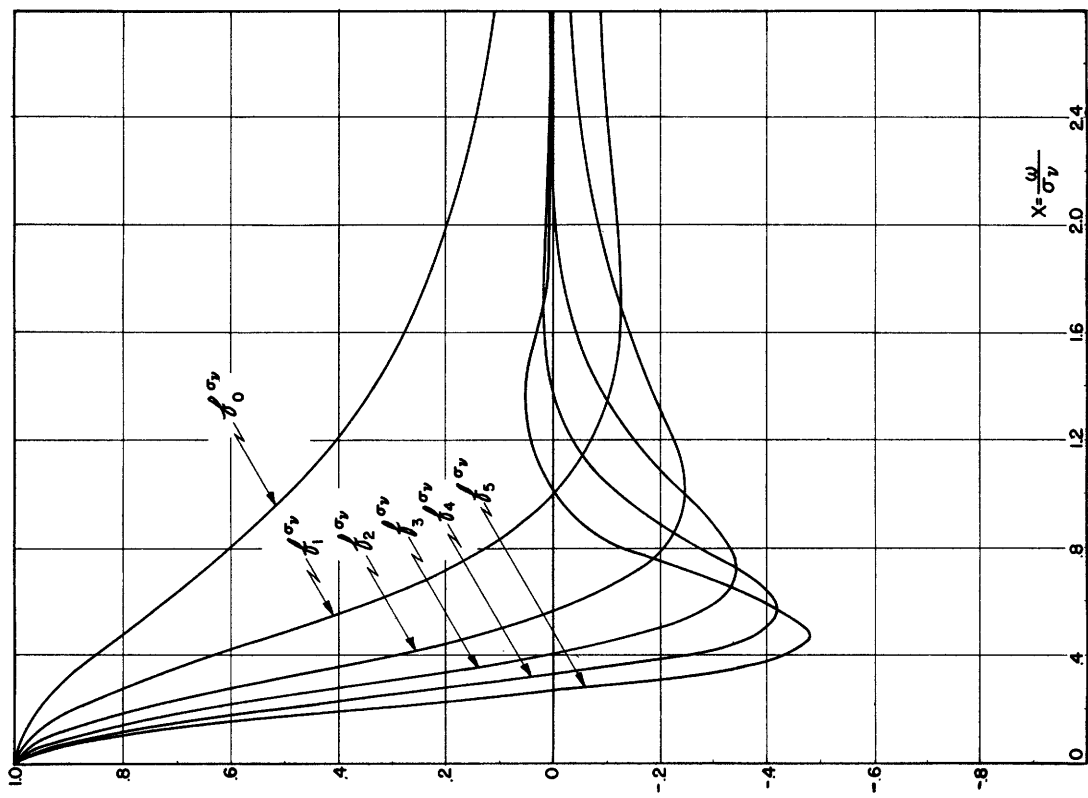


Figure 9. Weighting functions for zeros of transmission at  $\lambda_v = \pm \omega_v$ .

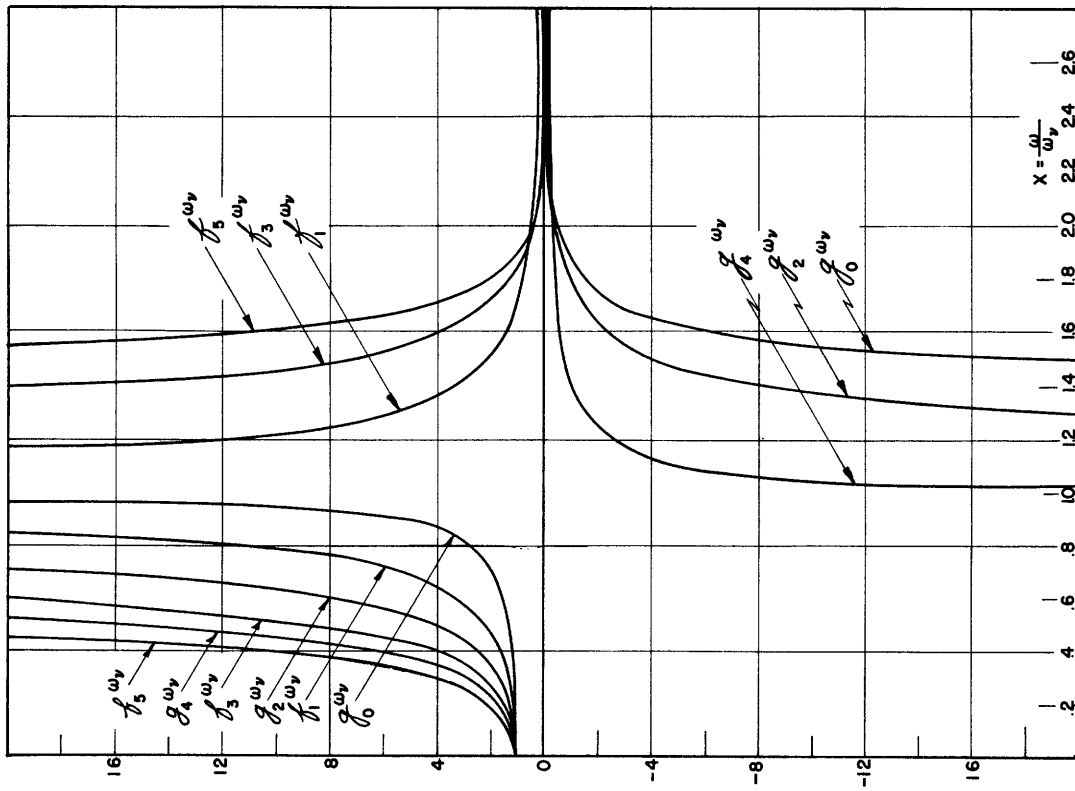


Figure 8. Weighting functions for zeros of transmission at  $\lambda_v = \pm j\omega_v$ .

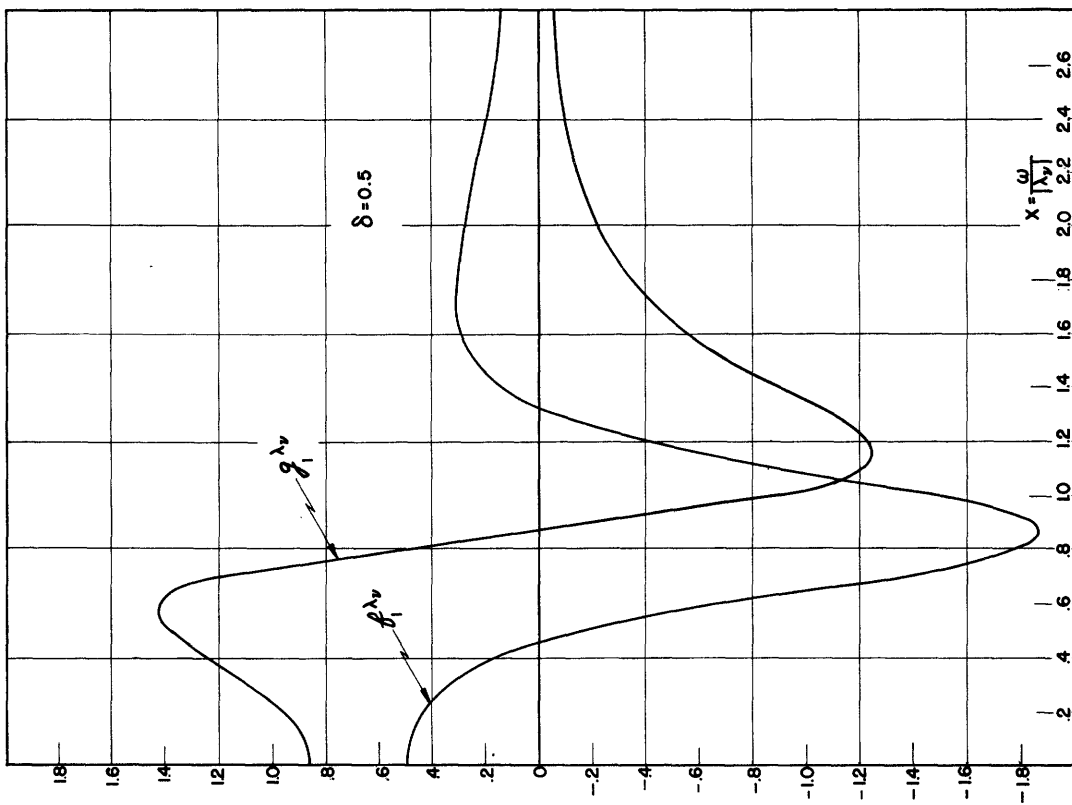


Figure 11. Weighting functions for zeros of transmission at  $\lambda_v = \pm \omega_v + j w_v$ .

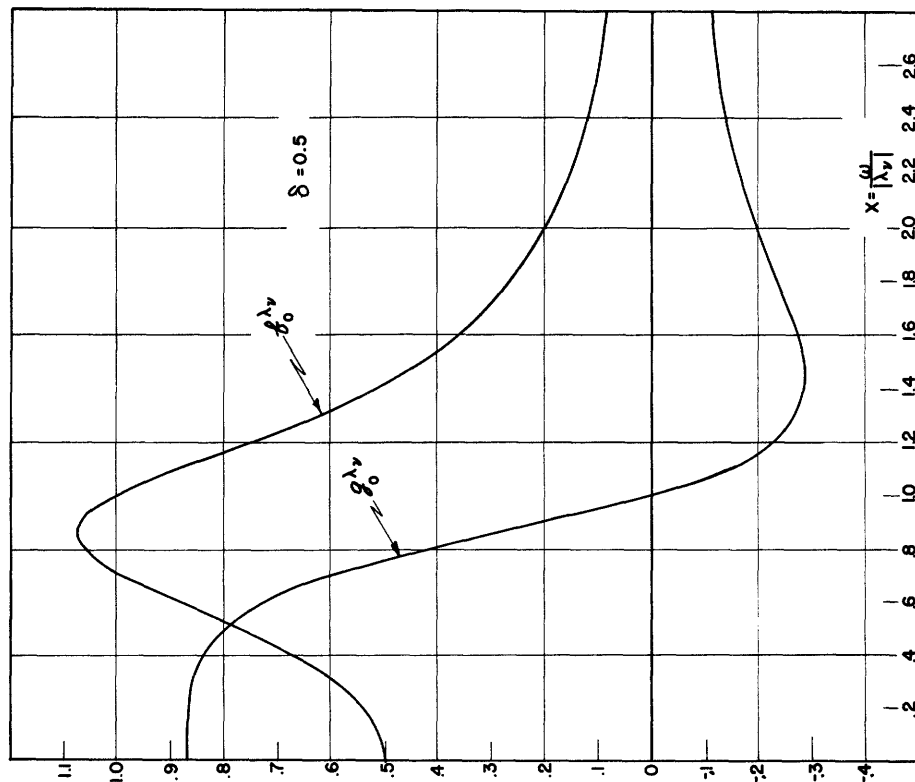


Figure 10. Weighting functions for zeros of transmission at  $\lambda_v = \pm \omega_v + j w_v$ .

Figure 13. Weighting functions for zeros of transmission at  $\lambda_p = \pm \sigma_p \pm j\omega_p$ .

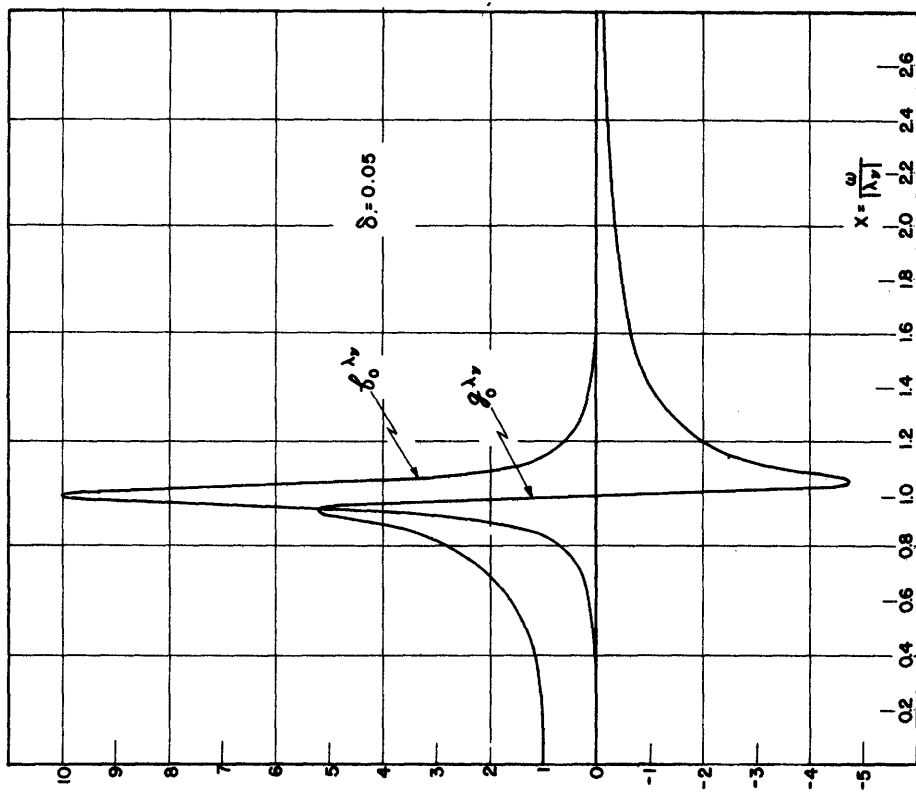
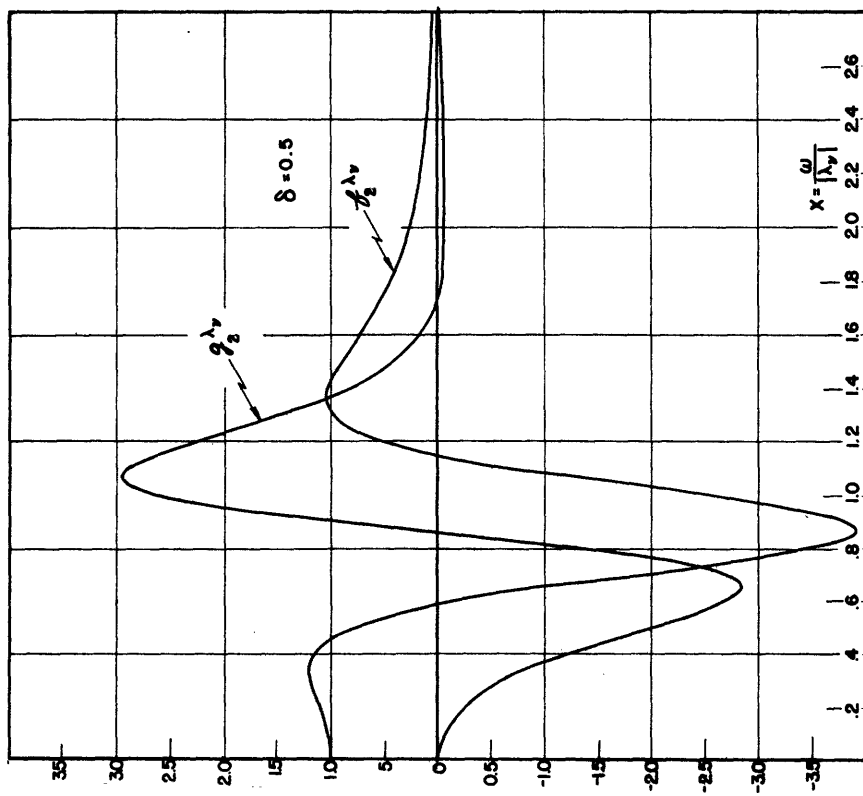


Figure 12. Weighting functions for zeros of transmission at  $\lambda_p = \pm \sigma_p \pm j\omega_p$ .



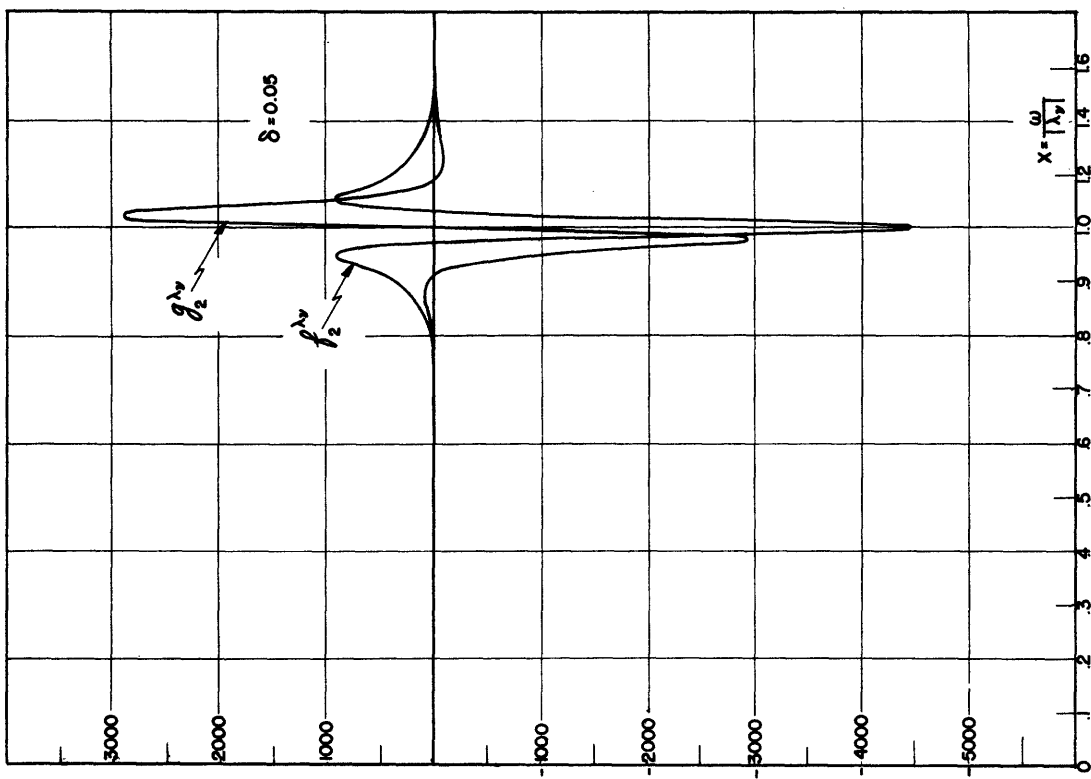


Figure 15. Weighting functions for zeros of transmission at  $\lambda_2 = \pm\sigma_2 + j\omega_2$ .

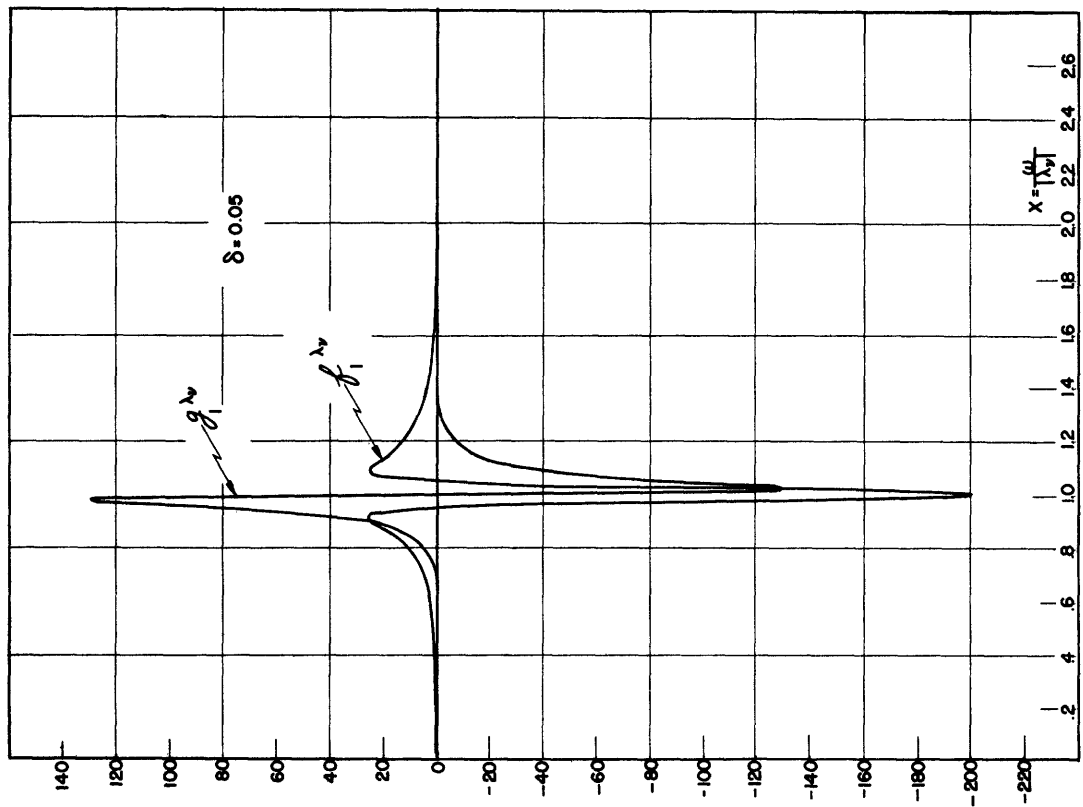


Figure 14. Weighting functions for zeros of transmission at  $\lambda_1 = \pm\sigma_1 + j\omega_1$ .

#### 4. The Design of Simple Matching Networks

The integral relations derived above indicate that the ideal type of behavior for the return loss at the input terminals of a matching network is represented by the rectangular-shaped function used in the determination of the optimum tolerance. Such a behavior cannot be obtained in practice because it requires a matching network with an infinite number of elements, but can be approximated sufficiently well for practical purposes by means of a reasonably small number of elements. In other words, the function representing  $|p_1|$  must be selected in such a way as to approximate a constant over the pass band and unity over the attenuation band, just as in the case of conventional filters. It must be pointed out, however, that filters are designed in most cases to provide a perfect match at a number of frequencies in the pass band, while such a situation is to be avoided in the case of matching networks. In fact, making  $\ln 1/|p_1|$  very large at any point of the pass band leads to an inefficient use of the areas represented by the integrals discussed above, and results, therefore, in a reduction of the bandwidth of approximate match. In spite of this essential difference between the characteristics of filters and matching networks, the same techniques can be used in both cases for the solution of the approximation problem. This point is made clear by the illustrative examples discussed below.

A very simple and important type of matching problem is presented by the case of a load impedance consisting of a resistance in series with an inductance, or by the dual case of a resistance shunted by a condenser. Practical problems of this type arise, for instance, in connection with the broadbanding of the high-frequency response of matching transformers, or when a resistive load is shunted by a stray capacitance. A method of designing appropriate matching networks for a series RL impedance is developed below. The same method will be directly applicable to the dual case of a shunt RC admittance.

The pass band desired in most of these problems extends from zero frequency to some cut-off frequency  $\omega_c$ ; the ideal behavior for the return loss is, therefore, that illustrated in Fig. 6. Let  $L_1$  be the value of the inductance normalized with respect to the series resistance, that is divided by it. The coefficient  $A_1^\infty$  is, by definition,

$$A_1^\infty = \left[ \frac{d}{d\lambda} \left( \ln \frac{2+\lambda L_1}{\lambda L_1} \right) \right]_{\substack{\lambda=0 \\ \lambda \rightarrow \infty}} = \frac{2}{L_1} . \quad (31)$$

The maximum theoretical pass-band value of  $\ln 1/|p_1|$  is, therefore, according to Eq. (24)

$$(\ln 1/|p_1|)_{\max} = \frac{\pi}{\omega_c L_1} . \quad (33)$$

The problem consists then of approaching this theoretical limit by means of a matching network involving a finite and prescribed number of elements.

The general remarks made above indicate that the inductance  $L_1$ , which forms the network  $N'$ , may be considered as the first element of a low-pass filter, the network  $N$ , whose input reflection coefficient is  $\rho_1$ . This reflection coefficient cannot be measured in practice, because the inductance  $L_1$  is inseparable from the resistive termination; its magnitude, however, is equal to the magnitude of the reflection coefficient  $\rho_2$  at the other terminals of the filter to which the generator will be connected in actual operation.

Two types of functions are used for the solution of the approximation problem in the case of low-pass filters<sup>3,8</sup>. The first type of function is the Tchebysheff polynomial  $T_n(w/w_c)$  which leads to a function  $|\rho_1|$  which oscillates between two given values in the pass band, and asymptotically approaches unity in the attenuation band, as illustrated in Fig. 16.

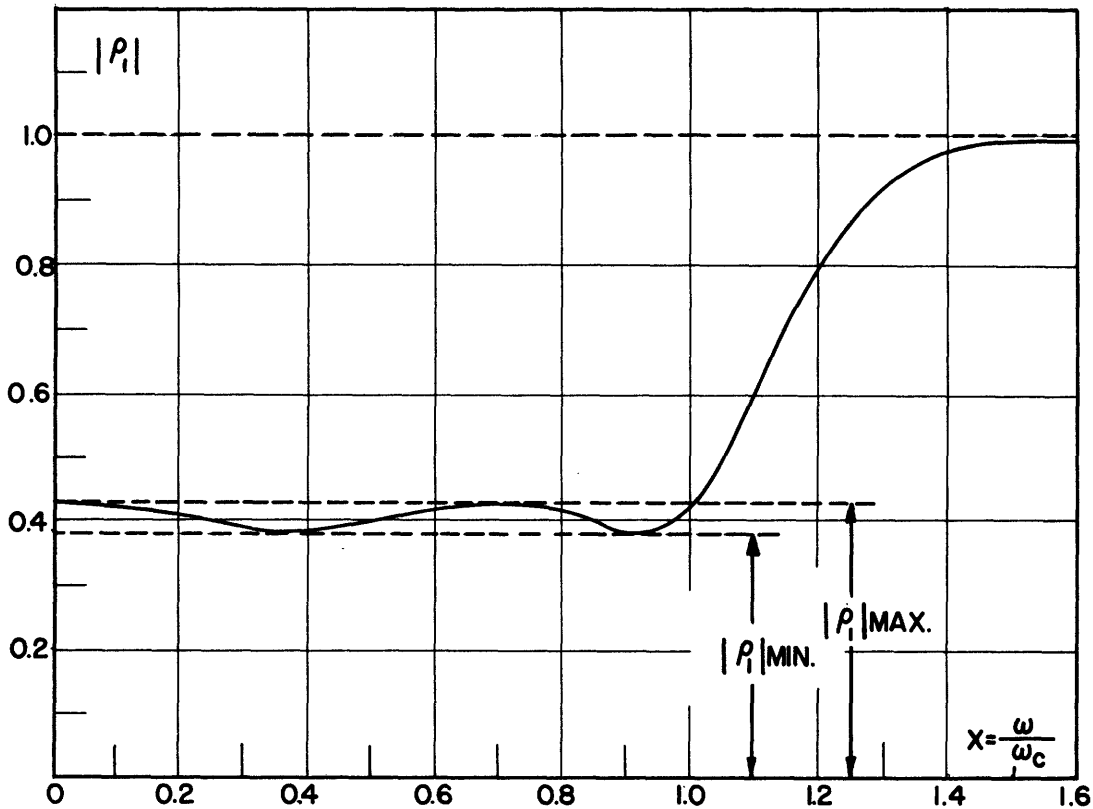


Figure 16. Typical frequency behavior of  $\rho_1$  with Tchebysheff approximation (computed for the network of Fig. II-1).

The second type of function is the Jacobian elliptic function which leads to an oscillatory behavior of  $|\rho_1|$  in both the pass band and the attenuation band. In the first case, all the zeros of transmission are at

infinity so that the network consists of a simple ladder structure with a total of  $n$  series inductances and shunt condensers. In the second case, zeros of transmission are present at finite frequencies as well as at infinity, and the resulting network has a form similar to the "m-derived" filters. The design involving elliptic functions leads to a slightly better tolerance, but the difference does not seem to be worth the resulting theoretical and practical complications.

The Tchebysheff polynomial of the first kind and order  $n$  is defined by

$$T_n(x) = \cos(n \cos^{-1} x).$$

It is clear that this function oscillates between plus and minus one for  $|x| < 1$ , and approaches  $\pm\infty$  for  $|x| > 1$ . In order to obtain the function  $|\rho_1|^2$ , one first constructs a function  $|t|^2$  which has oscillatory behavior in the pass band, is smaller than unity, and has all its zeros at infinity. Letting  $x = \omega/\omega_c$ , one obtains

$$1/|t|^2 = (1+K^2) + \epsilon^2 T_n^2(x),$$

where  $K$  and  $\epsilon$  are arbitrary constants. The corresponding magnitude of the reflection coefficient becomes, after appropriate manipulation.

$$|\rho_1|^2 = 1 - |t|^2 = [\rho_1(z)\rho_1(-z)]_{z=jx} = \begin{cases} \left[ \frac{\cosh n(\sinh^{-1} z-b)}{\cosh n(\sinh^{-1} z-a)} \frac{\cosh n(\sinh^{-1} z+b)}{\cosh n(\sinh^{-1} z+a)} \right]_{z=jx} & (n \text{ even}) \\ \left[ \frac{\sinh n(\sinh^{-1} z-b)}{\sinh n(\sinh^{-1} z-a)} \frac{\sinh n(\sinh^{-1} z+b)}{\sinh n(\sinh^{-1} z+a)} \right]_{z=jx} & (n \text{ odd}) \end{cases} \quad (34)$$

where  $z = \lambda/\omega_c$ ,  $\sinh^2 nb = (K/\epsilon)^2$ , and  $\sinh^2 na = (1+K^2)/\epsilon^2$ . The poles of this function are evidently given by

$$z_p = \begin{cases} \sinh \left[ \pm a \pm j \frac{\pi}{n} (m+\frac{1}{2}) \right] & (n \text{ even}) \\ \sinh \left[ \pm a \pm j \frac{\pi}{n} m \right] & (n \text{ odd}) \end{cases}, \quad (35)$$

where  $m$  is an integer or zero. The zeros are given by the same expression in which  $b$  is substituted for  $a$ . It will be noted that the poles lie on an ellipse centered at the origin with semiaxes equal to  $\cosh a$  and  $\sinh a$ , as indicated in Fig. 17 for the two cases of  $n=3$  and  $n=4$ . The zeros lie similarly on an ellipse of semiaxes equal to  $\cosh b$  and  $\sinh b$ .

The poles of  $\rho_1$  are necessarily those poles of  $[\rho_1(\lambda)\rho_1(-\lambda)]$  which lie in the left half-plane; that is,  $a$  must be taken with the

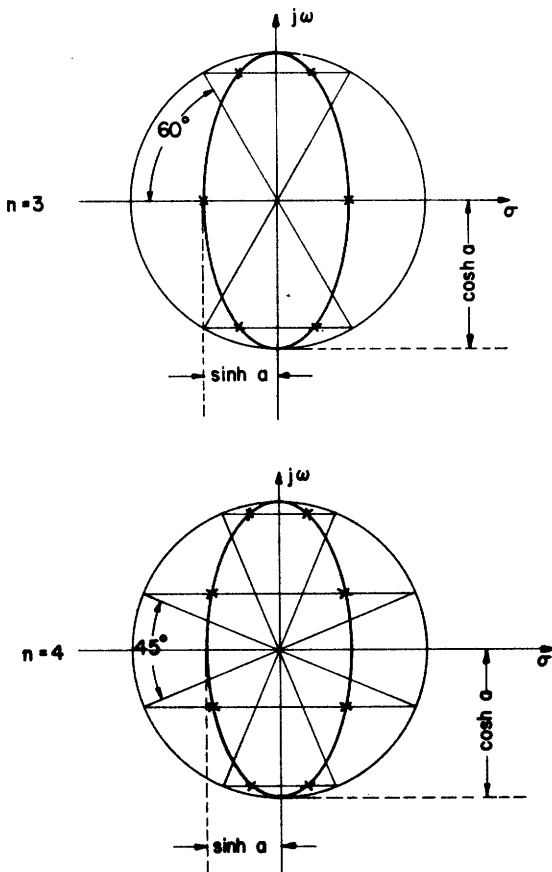


Figure 17. Location of the poles of  $\rho_1(\lambda)\rho_1(-\lambda)$  for a network with three or four elements.

negative sign. The zeros of  $\rho_1$ , on the contrary, can be located anywhere in the complex plane, as far as the physical realizability of the function is concerned. It has been shown before, however, that the area represented by  $\int \ln 1/|\rho_1| dw$  is a maximum for a given  $A_1^\infty$  when all the zeros of  $\rho_1$  are in the left half-plane. Therefore  $b$  must be taken also with the negative sign. The coefficient  $A_1^\infty$  corresponding to the resulting function  $\rho_1$  is then computed by means of Eq. (10) as follows

$$A_1^\infty = \sum_i (\lambda_{oi} - \lambda_{pi}) = \omega_c \frac{\sinh a - \sinh b}{\sin \pi/2n} \quad (36)$$

The quantities  $a$  and  $b$  must satisfy this equation since  $A_1^\infty$  is specified by the load impedance through Eq. (32). In addition,  $a$  and  $b$  must be chosen so as to minimize the tolerance of match. One obtains from Eq. (34)

$$|\rho_1|_{\max} = \frac{\cosh nb}{\cosh na} \quad (37)$$

This value is then minimized, subject to the condition imposed by Eq. (36),

by using the method of indeterminate multipliers. The result is

$$\frac{\tanh na}{\cosh a} = \frac{\tanh nb}{\cosh b} . \quad (38)$$

The parameters a and b are determined, finally, by solving simultaneously Eqs. (36) and (38). The resulting optimum value of  $\sinh a$  is plotted in Fig. 18 as a function of  $A_1^\infty/\omega_c$  for different values of  $n$  up to and including

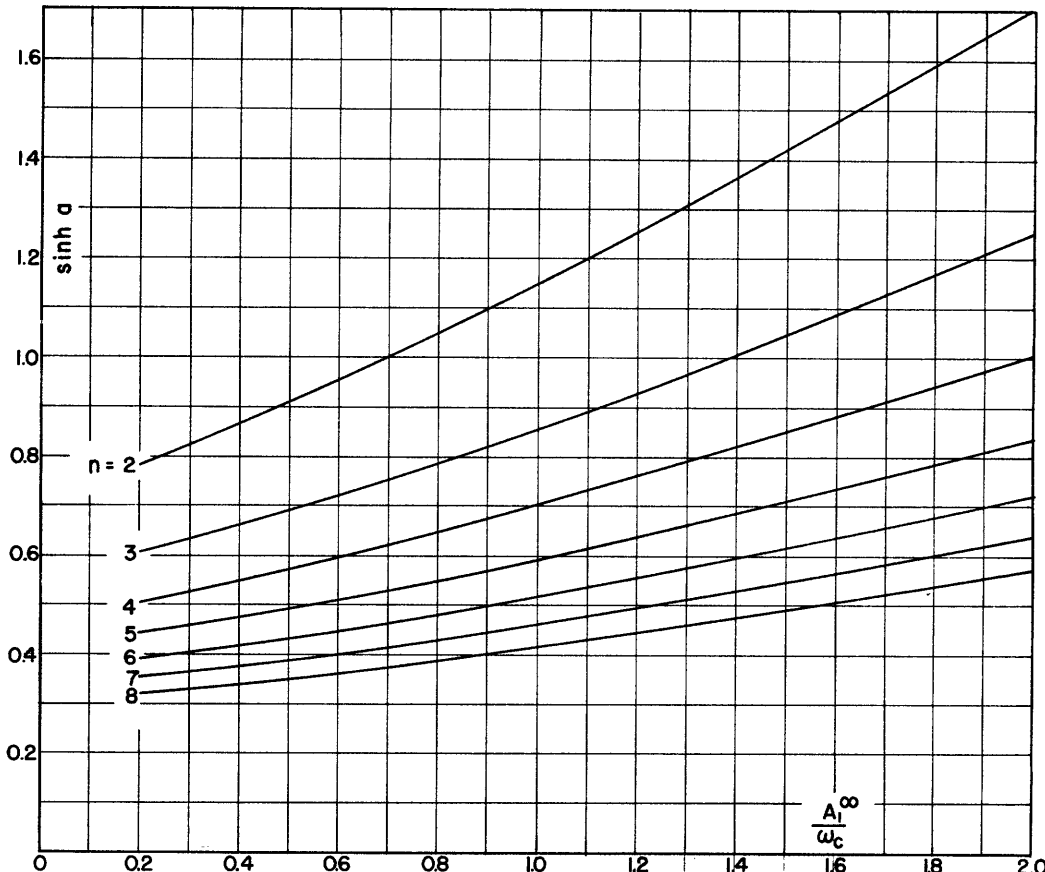


Figure 18. Design curves for a ladder network with  $n$  elements.

\* 8. The corresponding values of  $\sinh b$  can be obtained by means of Eq. (36).

The optimum value of the tolerance can be determined by means of Eq. (37). Figure 19 presents a plot of  $\ln 1/\rho_{11} \max$  as a function of  $A_1^\infty/\omega_c$  for different values of  $n$ . The curve indicated with  $n=\infty$  is the straight line of slope equal to  $\pi/2$  which represents the limiting value of the tolerance given by Eq. (24). It will be noted that this limiting value is approached reasonably well with a relatively small number ( $n-1$ ) of elements in the matching network. In the limit, when  $n$  approaches

---

\* These curves are obtained from computations made by Dr. M. Cerrillo, following a graphical procedure suggested by Dr. E. A. Guillemin.

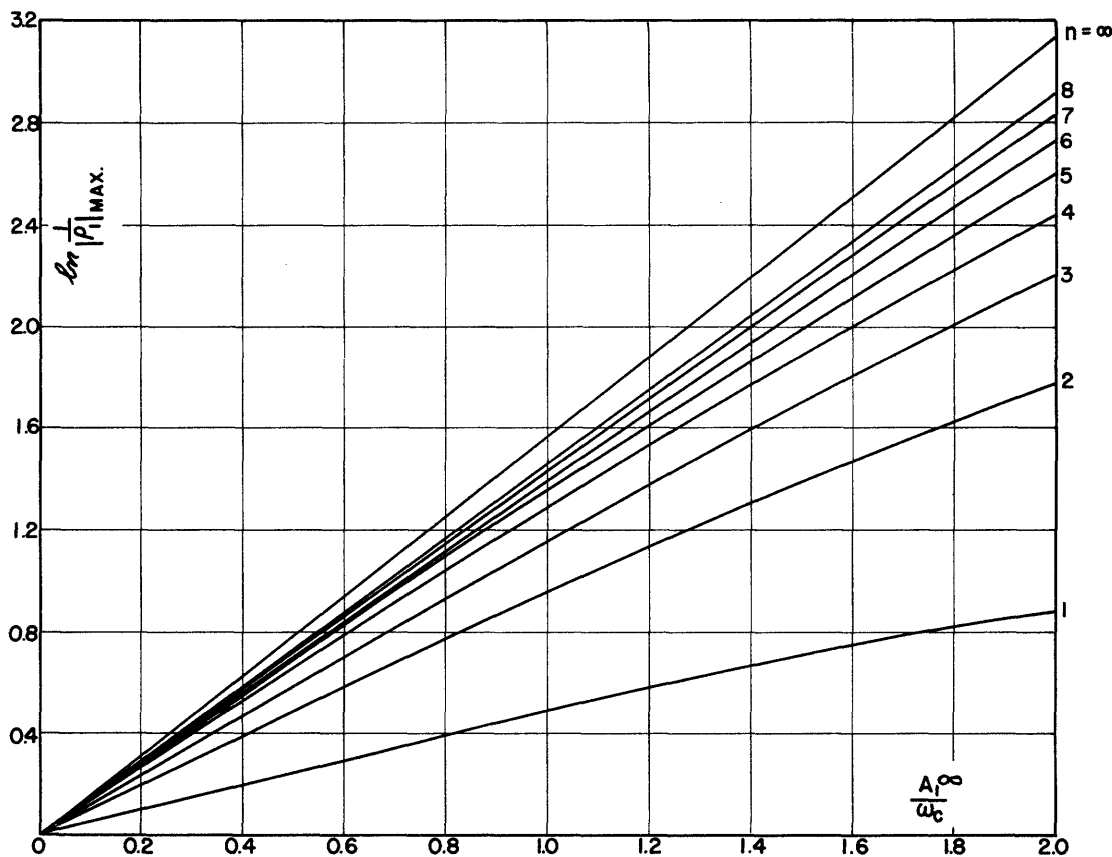


Figure 19. Tolerance of match for a low-pass ladder structure with  $n$  elements

infinity and both  $a$  and  $b$  approach zero as  $1/\sqrt{n}$ , Eqs. (36) and (37) yield Eq. (24), as one would expect.

After determining the function  $\rho_1$ , one can compute, finally, the values of the elements of the matching network. For this purpose, any one of the available synthesis procedures can be followed, a discussion of which is beyond the scope of this paper<sup>3,8</sup>. It seems appropriate, on the other hand, to mention a method of computing the element values developed by the author in connection with the matching problem. This method has the advantage of permitting direct and independent computation of the individual elements from the values of  $a$  and  $b$  determined above.

Consider a ladder structure consisting of series inductances and shunt condensers. The  $A^\infty$  coefficients can be computed from the poles and zeros of  $\rho_1$  by means of Eq. (10). On the other hand, the coefficient  $A_{2k-1}^\infty$  depends only on the first  $k$  elements of the ladder, so that the value of the  $k^{\text{th}}$  element depends only on the coefficients with subscript smaller than or equal to  $2k-1$ . It should be possible, therefore, to compute the values of the elements directly from the  $A^\infty$  coefficients, and these in turn from the values of the parameters  $a$  and  $b$ . Appropriate

equations have been derived for  $k=4$ , by computing the  $A^\infty$  for a ladder structure with 4 elements, and solving the resulting set of equations for the element values. The procedure is straightforward but very laborious, and therefore only the final results are given here.

Let the successive elements of the ladder be  $L_1, C_2, L_3, \dots$ , etc., and also let

$$\alpha_3 = 2^2 \frac{A_3^\infty}{(A_1^\infty)^3} - 1/3, \quad \alpha_5 = 2^4 \frac{A_5^\infty}{(A_1^\infty)^5} - 1/5, \quad \alpha_7 = 2^6 \frac{A_7^\infty}{(A_1^\infty)^7} - 1/7 \quad . \quad (39)$$

One has for the elements

$$L_1 = \frac{2}{A_1^\infty}, \quad C_2 = -\frac{L_1}{\alpha_3}, \quad L_3 = -\frac{\alpha_3 L_1}{1+\alpha_3-(\alpha_5/\alpha_3)}, \quad ,$$

$$C_4 = \frac{[1+\alpha_3-(\alpha_5/\alpha_3)]^2 L_1}{\alpha_3 [1+\alpha_3-(\alpha_5/\alpha_3)+(\alpha_5/\alpha_3)^2-(\alpha_7/\alpha_3)]} \quad . \quad (40)$$

In the particular case of the functional form for  $\rho_1$  discussed above, one obtains by means of Eq. (10)

$$A_3^\infty = -2^{-2} \omega_c^3 \left( \frac{\sinh 3a - \sinh 3b}{3 \sin(3\pi/2n)} + \frac{\sinh a - \sinh b}{\sin(\pi/2n)} \right) \quad , \quad (41)$$

$$A_5^\infty = 2^{-4} \omega_c^5 \left( \frac{\sinh 5a - \sinh 5b}{5 \sin(5\pi/2n)} + \frac{\sinh 3a - \sinh 3b}{\sin(3\pi/2n)} + \right. \\ \left. + 2 \frac{\sinh a - \sinh b}{\sin(\pi/2n)} \right), \quad (42)$$

$$A_7^\infty = -2^{-6} \omega_c^7 \left( \frac{\sinh 7a - \sinh 7b}{7 \sin(7\pi/2n)} + \frac{\sinh 5a - \sinh 5b}{\sin(5\pi/2n)} + \right. \\ \left. + 3 \frac{\sinh 3a - \sinh 3b}{\sin(3\pi/2n)} + 5 \frac{\sinh a - \sinh b}{\sin(\pi/2n)} \right). \quad (43)$$

It will be noted that the equations given above are sufficient for the design of a structure with 8 elements. In fact 4 elements can be computed by operating from one end of the network and the other four by operating from the other end. The reflection coefficient  $\rho_2$  which must be used in the second part of the design can be obtained from  $\rho_1$  in a simple manner, as indicated in Appendix I. One must keep in mind, however, that the

network will, in general, involve an ideal transformer, since both terminations are assumed to be equal to one ohm. The turns ratio of the transformer can be determined easily from the zero-frequency behavior of the network. Illustrative examples are presented in Appendix II.

Next consider the design of a matching network for a load impedance consisting of a capacitance shunting a series RL combination. A problem of this type may arise in connection with the high-frequency response of step-up transformers, as discussed in Appendix III. The limiting tolerance for this matching problem is given by the curves in Fig. 7. This optimum tolerance was obtained by introducing a zero of  $\rho_1$  at a point  $\sigma_r$  of the positive real axis together with a symmetrical pole on the negative real axis. The same technique is used in obtaining the appropriate function for  $\rho_1$  when the matching network must contain a specified number of elements. Also the same approximation function can be used for  $|\rho_1|$  as in the case discussed above, because the addition of a zero and a pole symmetrically located with respect to the imaginary axis leaves the value of  $|\rho_1|$  unchanged for imaginary values of  $\lambda$ . One obtains, in this case, from the conditions of physical realizability for  $\rho_1$ ,

$$A_1^\infty / \omega_c = 2/\omega_c L_1 = \frac{\sinh a - \sinh b}{\sin(\pi/2n)} + 2\sigma_r/\omega_c , \quad (44)$$

$$- A_3^\infty / \omega_c^3 = 2^{-2} (A_1^\infty / \omega_c)^3 (L_1/C_2 + 1/3) = \quad (45)$$

$$= 2^{-2} \left( \frac{\sinh 3a - \sinh 3b}{3 \sin(3\pi/2n)} + \frac{\sinh a - \sinh b}{\sin(\pi/2n)} \right) - 2/3 (\sigma_r/\omega_c)^3 .$$

The maximum pass-band value of  $|\rho_1|$  is still given by

$$|\rho_1|_{\max} = \frac{\cosh nb}{\cosh na} . \quad (46)$$

The parameters  $a$ ,  $b$ , and  $\sigma_r$  must be determined in such a way as to minimize the value of  $|\rho_1|_{\max}$  and satisfy, at the same time, the equations above. This minimization process involves the solution of a system of transcendental equations. No convenient graphical procedure could be developed in this case.

Once  $a$ ,  $b$ , and  $\sigma_r$  have been determined, the values of the elements can be computed by following a procedure very similar to the one discussed above, but in this case a Darlington section of type C (see Fig. III-2) is present in addition because of the zero of transmission at  $\lambda = \sigma_r$ . An illustrative design is carried out in Appendix III.

The design of matching networks for impedances of a more complex nature than those considered above is hampered in most cases by mathematical difficulties which lead to laborious numerical and graphical computations. It must be said, however, that many matching problems of practical interest are of the types discussed above, or can be reduced to these types by means of simple changes of the frequency variable. In addition, a rigorous method of design can at times be combined effectively with a cut-and-try procedure. For instance, the frequency behavior of a given load impedance might first be modified empirically in such a way as to approximate, over the desired frequency band, the behavior of a simpler impedance function for which a rigorous design procedure is available. In such cases the ingenuity of the designer becomes of primary importance, since the technique to be used may vary considerably from one type of problem to another.

ACKNOWLEDGMENT. I wish to express my deep and sincere gratitude to Professor E. A. Guillemin, who supervised this work, for his constant advice and encouragement. In addition, and above all, I owe to his inspired teaching the knowledge of network theory on which the entire work presented in this paper is based.

#### REFERENCES

1. R. M. Fano and A. W. Lawson, Jr., "Microwave Filters Using Quarter-Wave Couplings", Proc. I.R.E. Vol. 35, No. 11, pp. 1318-1323, Nov. (1947); also RLE Technical Report No. 8.
2. E. A. Guillemin, "Communication Networks", Vol. II, Ch. X, Sec. 13, Wiley, New York (1935).
3. S. Darlington, "Synthesis of Reactance 4-Poles", Journal of Mathematics and Physics, Vol. XVIII, pp. 275-353, September 1939. Also Bell Telephone System Monograph B-1186.
4. H. W. Bode, "A Method of Impedance Correction", B.S.T.J., Vol. IX, pp. 794-835, October 1930.
5. E. A. Guillemin, op. cit., Ch. IX, Sec. 12.
6. H. W. Bode, "Network Analysis and Feedback Amplifier Design", Sec. 16.3, Van Nostrand, New York, 1945.
7. H. W. Bode, op. cit., Secs. 10.7 and 10.8.
8. R. M. Fano and A. W. Lawson, Jr., "The Theory of Microwave Filters", Ch. 9, Vol. 9, Radiation Laboratory Series, McGraw-Hill, New York, (in press).

## APPENDIX I

The reflection and transmission coefficients of a two-terminal-pair reactive network represent the characteristics of the network when one-ohm terminations are connected to both pairs of terminals, as shown in Fig. I-1. The two reflection coefficients are defined by

$$\rho_1 = \frac{Z_1 - 1}{Z_1 + 1} = \left[ \frac{2V_1}{E_1} - 1 \right]_{E_2=0}, \quad (I-1)$$

$$\rho_2 = \frac{Z_2 - 1}{Z_2 + 1} = \left[ \frac{2V_2}{E_2} - 1 \right]_{E_1=0}, \quad (I-2)$$

where  $Z_1$  and  $Z_2$  are the impedances measured at the two pair of terminals when the voltage sources are short-circuited. The transmission coefficient is defined, with reference to Fig. I-1, by

$$t = \left[ \frac{2V_2}{E_1} \right]_{E_2=0} = \left[ \frac{2V_1}{E_2} \right]_{E_1=0}. \quad (I-3)$$

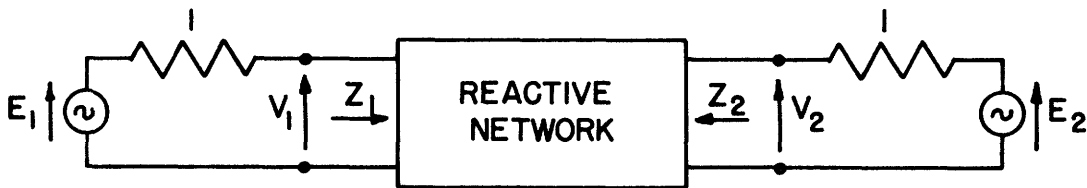


Figure I-1. Two-terminal-pair reactive network with one-ohm terminations.

The physical significance of these coefficients is best understood by inserting two transmission lines of unit characteristic impedance between the network and the terminations. The reflection coefficient  $\rho_1$  is then the ratio of the voltage of the reflected wave to the voltage of the incident wave measured at terminals 1 for  $E_2=0$ ;  $\rho_2$  has the same significance for terminals 2. The transmission coefficient  $t$  is the ratio of the voltage of the transmitted wave at terminals 2 to the voltage of the incident wave at terminals 1, for  $E_2=0$ . Because of the reciprocity theorem, the same value of  $t$  is obtained for transmission in the opposite direction.

It is clear from the above definitions that  $|\rho_1|^2$  is the per unit power reflected and  $|t|^2$  is the per unit power transmitted. Since the

network is non-dissipative, one obtains

$$|\rho_1|^2 = |\rho_2|^2 = 1 - |t|^2 . \quad (I-4)$$

This equation implies that any function of the complex variable  $\lambda = \sigma + j\omega$  which is to represent a reflection or transmission coefficient must have a magnitude smaller than, or equal to, unity at all points of the imaginary axis, that is at real frequencies. In addition, all the poles of this function must lie in the left half of the complex plane, because, otherwise, the network would oscillate upon any random disturbance. It can be shown<sup>3,8</sup> that this condition on the poles together with the condition on the magnitude on the imaginary axis are sufficient as well as necessary conditions for the physical realizability of a reflection coefficient. In the case of a transmission coefficient, one must add the condition that the zeros be present in pairs symmetrical with respect to the imaginary axis<sup>3,8</sup>. It is understood, of course, that any reflection or transmission coefficient of a lumped-element network must be the ratio of two real polynomials in the complex variable  $\lambda$ .

If the reflection coefficient  $\rho_1$  of a network is written in the form

$$\rho_1(\lambda) = K \frac{(\lambda - \lambda_{o1})(\lambda - \lambda_{o2}) \dots (\lambda - \lambda_{on})}{(\lambda - \lambda_{p1})(\lambda - \lambda_{p2}) \dots (\lambda - \lambda_{pn})} , \quad (I-5)$$

it can be shown that the reflection coefficient  $\rho_2$  is given by

$$\rho_2(\lambda) = (-1)^{n+1} K \frac{(\lambda + \lambda_{o1})(\lambda + \lambda_{o2}) \dots (\lambda + \lambda_{on})}{(\lambda - \lambda_{p1})(\lambda - \lambda_{p2}) \dots (\lambda - \lambda_{pn})} . \quad (I-6)$$

The  $\lambda_{oi}$  and the  $\lambda_{pi}$  are, respectively, the zeros and poles of  $\rho_1$ ;  $K$  is a real constant.

A relation between the reflection coefficients and  $t$  can be obtained by noting that

$$[\rho_1(\lambda) \rho_1(-\lambda)]_{\lambda=j\omega} = |\rho_1|^2_{\lambda=j\omega} = [\rho_2(\lambda) \rho_2(-\lambda)]_{\lambda=j\omega} = |\rho_2|^2_{\lambda=j\omega} \quad (I-7)$$

and

$$[t(\lambda) t(-\lambda)]_{\lambda=j\omega} = |t|^2_{\lambda=j\omega} = 1 - |\rho_1|^2_{\lambda=j\omega} . \quad (I-8)$$

It follows that the reflection and transmission coefficients have the same denominator, and therefore the same poles. The numerator of  $t$  is either an even or an odd polynomial, because the zeros of  $t$  must be present in pairs of quadruplets symmetrical with respect to the origin. It follows that the numerator of  $[t(\lambda)t(-\lambda)]$  must be a perfect square; that is, its zeros must have even multiplicity. It must be pointed out in this regard that the function computed from either reflection coefficient by means of Eq.(I-8) might not satisfy this requirement. In such a case it is necessary to multiply both the numerator and the denominator of the function  $[t(\lambda)t(-\lambda)]$  by the root factors of the numerator having odd multiplicity<sup>3,8</sup>. These root factors must be carried back into  $\rho_1$  and  $\rho_2$ , in which they will appear after appropriate eliminations as pairs of zeros in the right half-plane together with symmetrical pairs of poles in the left half-plane. Such quadruplets of singularities do not change the magnitude of the reflection coefficient on the imaginary axis, but introduce only a phase shift. A corresponding elimination of zeros and poles in the left half-plane will take place in the transmission coefficient. In some cases  $t$  contains a phase-shift factor, consisting of zeros in the right half-plane, and symmetrical poles in the left half-plane, and  $\rho_2$  contains the same factor squared while such a factor is missing in  $\rho_1$ . This situation indicates that an all-pass network of unit characteristic impedance is connected at terminals 2 of the network so as to introduce a phase shift in both  $t$  and  $\rho_2$  without affecting  $\rho_1$ .

It can be concluded on the basis of the above discussion that a two-terminal-pair reactive network is completely specified by either reflection coefficient, apart from an arbitrary all-pass phase-shift network connected in cascade at the opposite terminals.

## APPENDIX II

A convenient example for illustrating the method of designing matching networks for series RL or shunt RC impedances is the high-frequency broadbanding of a matching transformer. Suppose a transformer is to be used to match a low-impedance resistive load to a high-impedance generator. The transformer is known to behave at high frequency as an inductance  $L$  (leakage inductance) in series with the load resistance  $R_L$ . Let  $\omega_h = 2R_L/L$  be the half-power angular frequency of the transformer when the load is matched to the generator at low frequencies. It is desired to broadband this transformer so as to make the loss smaller than 1 db up to a frequency  $\omega_c = 3\omega_h/2$ . Incidental dissipation will be neglected in this example.

It is convenient to normalize the network to 1 ohm impedance level, in which case the normalized inductance becomes  $L_1 = L/R_L$ . One has then, from Eq. (32),

$$\tilde{A}_1^{\infty}/\omega_c = 2/3 . \quad (\text{II-1})$$

A transmission loss of 1 db corresponds to a value  $\ln 1/|\rho_1| = 0.79$ . Figure 19 shows that the optimum tolerance for  $\ln 1/|\rho_1|$  is 1.04, and that a value of 0.86 can be obtained with  $n=4$ , that is, with a matching network consisting of two capacitances and one inductance. The corresponding value of  $|\rho_1|_{\max}$  is 0.424 and the resulting transmission loss is 0.86 db. One obtains then from Fig. 18 and Eq. (36).

$$\begin{aligned} \sinh a &= 0.615, & a &= 0.582, \\ \sinh b &= 0.363, & b &= 0.356. \end{aligned} \quad (\text{II-2})$$

The corresponding function  $|\rho_1|$  is plotted in Fig. 16 versus the normalized frequency variable  $x = \omega/\omega_c$ .

In computing the element values one obtains from Eqs. (39)-(43)

$$a_3 = -4.493, \quad a_5 = 34.05, \quad a_7 = -435.1 , \quad (\text{II-3})$$

$$C_2 = 0.2225 L_1, \quad L_3 = 1.10 L_1, \quad C_4 = 0.1043 L_1. \quad (\text{II-4})$$

The turns ratio of the ideal transformer is specified by the zero-frequency value of  $|\rho_1|$ , that is, in this case, by  $|\rho_1|_{\max}$ . One has then

$$\text{turns ratio} = \sqrt{\frac{1+0.424}{1-0.424}} = 1.57 . \quad (\text{II-5})$$

The resulting network for 1-ohm impedance level is shown in Fig. II-1(a). In practice, the ideal transformer is combined with the matching transformer by performing a suitable change of impedance level. Figure II-1(b) shows the final network for a half-power frequency  $\omega_c = 50,000$  rad/sec, a load impedance of 10 ohms and a source impedance of 1000 ohms.

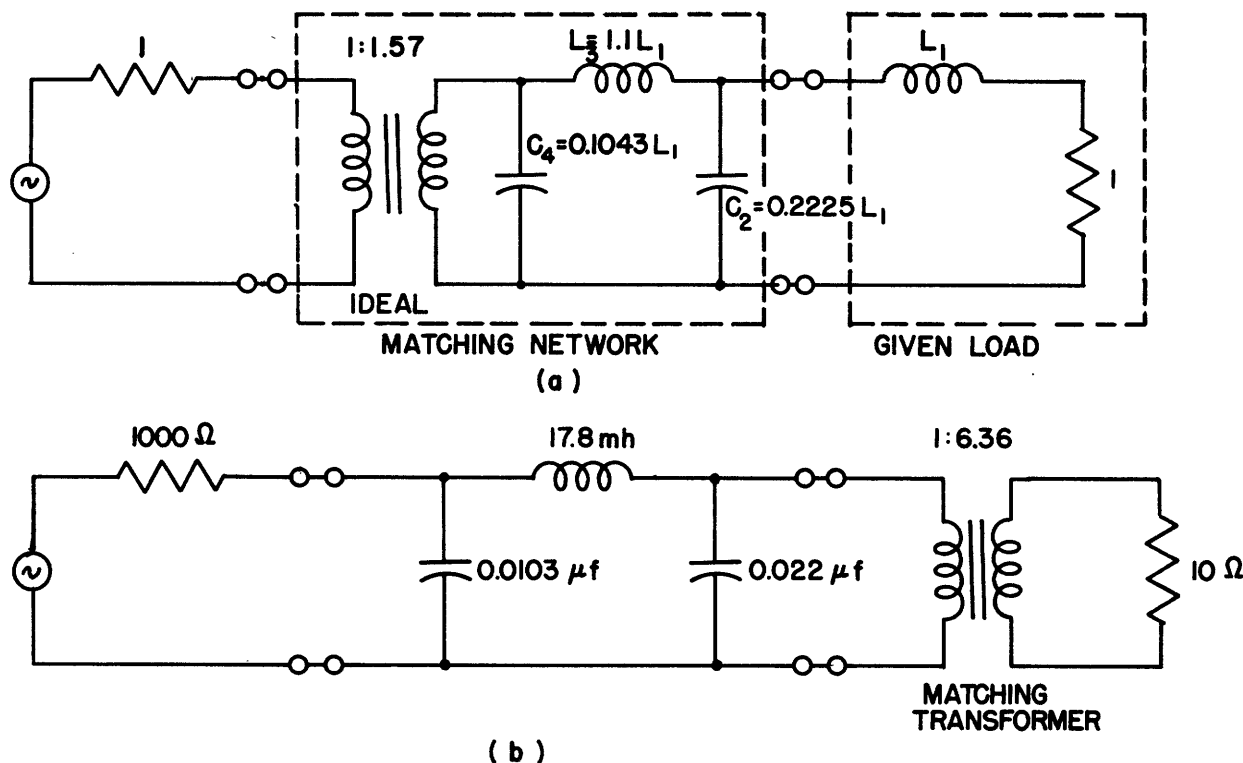


Figure II-1. Networks for the high-frequency broadbanding of a matching transformer.

The same design technique can be applied to the case of a load consisting of a series (or parallel) tuned circuit if the frequency band over which the load is to be matched is centered at the resonance frequency  $\omega_0$  of the tuned circuit. A practical example is offered by the broadbanding of a quarter-wave grounded antenna which behaves, to a first approximation, as a series tuned circuit. Suppose, for instance, that an antenna with radiation resistance of 30 ohms, resonance frequency of 10 Mc/sec, and Q of 10 is to be matched to a 50-ohm transmission line over a 3-Mc/sec band with a loss smaller than 1 db. When this band-pass problem is reduced to the equivalent low-pass problem, the same design data are obtained as in the previous example, and therefore the same basic matching network.

Figure II-2 shows the network obtained by transforming the basic low-pass structure of the previous example into the appropriate band-pass structure with the required impedance level. This network can be transformed further into a chain of tuned coupled coils, and appropriate changes of impedance level can be performed so as to eliminate the ideal transformer.

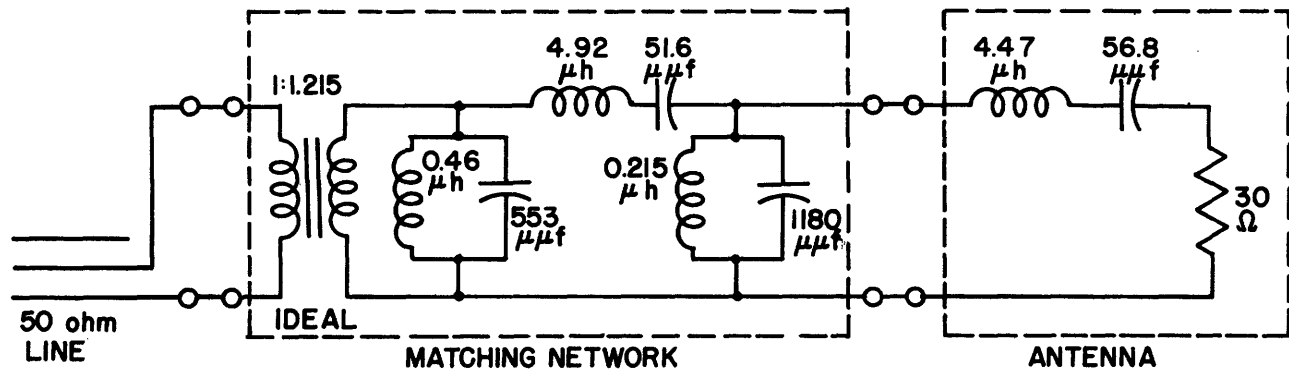
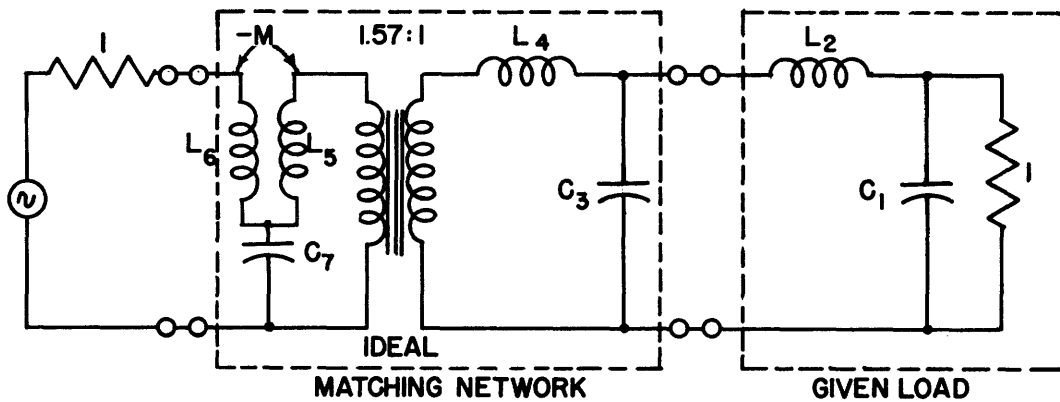


Figure II-2. Matching network for a resonant antenna.

### APPENDIX III

The broadbanding of the high-frequency response of a step-up transformer forms a convenient example of the technique used in matching a load impedance consisting of an inductance  $L$  in series with a parallel RC combination. In this case  $R$  is the load resistance,  $C$  is the stray capacitance of the secondary coil, and  $L$  is the total leakage inductance, all of them referred to the primary of the transformer. With reference to Fig. III-1, suppose the normalized values of the elements forming the load



$$C_1 = \frac{1.205}{\omega_c}, \quad L_2 = \frac{2.3}{\omega_c}, \quad C_3 = \frac{0.813}{\omega_c}, \quad L_4 = \frac{3.37}{\omega_c}$$

$$L_5 = \frac{0.66}{\omega_c}, \quad L_6 = \frac{1.135}{\omega_c}, \quad M = \sqrt{L_5 L_6}, \quad C_7 = \frac{4.63}{\omega_c}$$

Figure III-1. High-frequency broadbanding of a matching transformer with stray capacitance loading.

impedance are given by

$$C_1 = 1.205/\omega_c, \quad L_2 = 2.3/\omega_c,$$

where  $\omega_c$  is the upper limit of the frequency band over which the impedance is to be matched. One obtains from Eqs. (44) and (45), after interchanging  $C$  and  $L$ ,

$$\tilde{A}_1^\infty/\omega_c = 1.66, \quad -\tilde{A}_3^\infty/(\tilde{A}_1^\infty)^3 = 0.0475, \quad -\tilde{A}_3^\infty/\omega_c^3 = 0.217.$$

The optimum tolerance for  $\ln 1/|\rho_1|$  is given by the curves of Fig. 7 as 1.32, to which correspond a value of  $|\rho_1|_{\max}$  equal to 0.275.

To obtain the proper value of  $\sinh a$ , one should minimize the value of  $|\rho_1|_{\max}$  of Eq. (46) subject to the conditions imposed by Eqs. (44) and (45). To avoid this tedious computation, there will be assumed for  $\sinh a$  the same value that would be obtained if  $L_2$  were not a part of the specified load impedance. In addition the data of the problem have been selected, for the sake of simplicity, to yield for  $n=4$  the same values of  $a$  and  $b$  as in the example discussed in Appendix II, so that the maximum value of  $|\rho_1|$  is still 0.424 corresponding to  $\ln 1/|\rho_1|_{\max}=0.86$ . The corresponding value of  $\sigma_r/w_c$  is 0.5.

The next step in the design is the computation of the quantities  $a_3$ ,  $a_5$ ,  $a_7$ . In this case the quantities  $\frac{2}{5}\sigma_r^5$  and  $\frac{2}{7}\sigma_r^7$  must be added to the right-hand sides of Eqs. (41) and (42) to take into account the zero of  $\rho_1$  at  $\sigma_r$  and the pole at  $-\sigma_r$ . One obtains

$$a_3 = -0.523, \quad a_5 = 0.156, \quad a_7 = -0.666 .$$

The values of  $C_3$  and  $L_4$  in Fig. III-1 are computed by means of Eqs. (40), with due regard again to the fact that  $C$  and  $L$  must be interchanged because the first element of the ladder is, in this case, a capacitance instead of an inductance. It results that

$$C_3 = 0.813/w_c, \quad L_4 = 3.37/w_c .$$

The ratio of the ideal transformer is still 1.57, as in the case considered in Appendix II, but the transformer is reversed in direction because the dual network is being designed; that is, impedance has been interchanged with admittance.

In addition to the elements already computed, the presence of a zero of transmission of the matching network at  $-\sigma_r$  (resulting from the zero-pole pair of  $\rho_1$ ) leads to a Darlington section of type C illustrated in Fig. III-2. To determine the elements of this section it is convenient to operate on the reflection coefficient  $\rho_2$ , that is, from the opposite end of the network. It can be seen by inspection that if  $M$  is a positive quantity,

$$MC_7 = 1/\sigma_r^2 = 1/4w_c^2 .$$

At the same time, the reflection coefficient  $\rho_2$  must have a zero at  $\sigma_r$  and therefore the impedance measured at the  $L_6$  terminals must be one for

$\lambda = \sigma_r$ . It follows that

$$\sigma_r L_6 + 1/(\sigma_r C_7) = 1,$$

$$\sigma_r = (1/2L_6) [1 \pm \sqrt{1 - (4L_6/C_7)}].$$

The + sign must be used when  $\rho_2(\lambda + \sigma_r)/(\lambda - \sigma_r)$  is positive for  $\lambda = \sigma_r$ . The third equation required for the determination of the three elements is obtained by considering the quantity (see Eq. (16))

$$A_o = \ln \frac{\lambda - \sigma_r}{\rho_2(\lambda + \sigma_r)} - j\beta$$

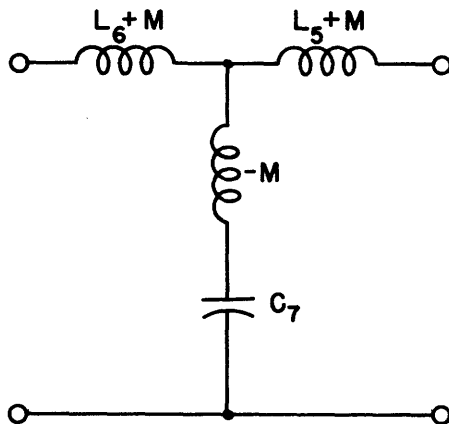


Figure III-2. Darlington section of type C for a zero of transmission on the real axis.

which is completely determined by the elements of the section. One obtains also, from Fig. III-2,

$$A_o = -\frac{1}{2} \ln (1 - 4L_6/C_7).$$

The numerical value of  $A_o$  is found to be -2. Remembering that  $L_5 L_6 = M^2$  one has finally

$$L_6 = 1.135/\omega_c, \quad L_5 = 0.66/\omega_c, \quad M = 0.865/\omega_c, \quad C_7 = 4.63/\omega_c.$$

The ideal transformer can be moved to the end of the structure and combined with the actual transformer, so that the load resistance

measured from the primary side and normalized with respect to the source resistance will be equal to  $1.57^2 = 2.47$  ohms. Finally, the coupling coefficient of the transformer in the section of type C is made smaller than unity by combining the transformer with the adjacent inductance  $L_4$ . The final network is shown in Fig. III-3, in which the values of all elements are normalized with respect to the source resistance.

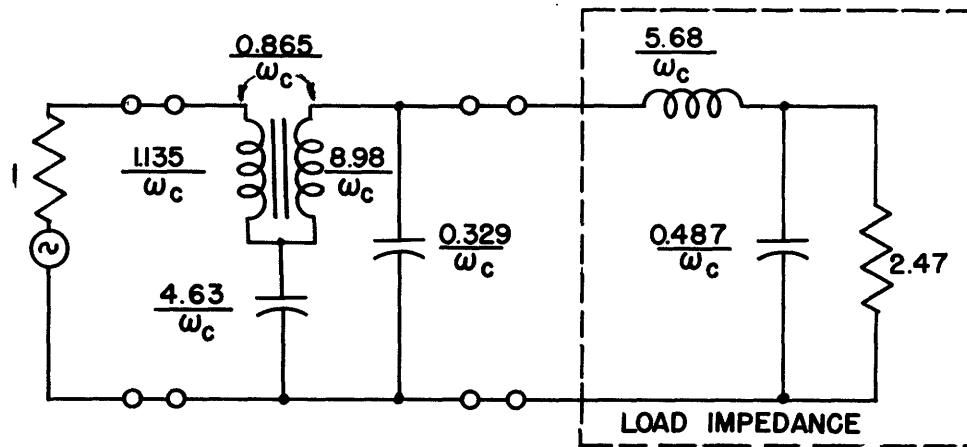


Figure III-3. Transformation of the network shown in Fig. III-1.